Spatiotemporal Evolution of Urban Thermal Conditions, Vegetation Dynamics, and Built-up Expansion in Ahmedabad, India (2000–2025) Using Multi-Temporal Landsat Analysis

Stephen Mekwan
Independent Researcher, India
Email: macwan008@gmail.com
ORCID: https://orcid.org/0000-0001-5249-3167

Peer review status:
This is a non-peer-reviewed preprint submitted to EarthArXiv.

Abstract: Rapid urban expansion has substantially altered urban thermal conditions across many semi-arid cities. This study examined spatiotemporal variation in land surface temperature (LST), vegetation cover, and built-up intensity across Ahmedabad, India, between 2000 and 2025 using multi-temporal Landsat imagery and the Google Earth Engine (GEE) platform. Spatial analysis revealed progressive expansion of high-temperature urban zones and increasing intra-urban thermal heterogeneity, particularly across densely urbanised eastern and central sectors of the city. Mean LST increased from 46.11°C in 2000 to 51.60°C in 2020 before declining during the 2025 acquisition period. Regression and correlation analyses indicated persistent negative relationships between vegetation cover and LST, whereas built-up intensity remained positively associated with elevated thermal conditions. Temporal analyses further suggested increasingly heterogeneous vegetation-temperature relationships through time, with later years exhibiting broader thermal variability across comparable NDVI ranges despite localised increases in vegetation cover. The final multivariate regression model explained substantial variation in LST (Adjusted $R^2 = 0.690$). Overall, the findings indicate that continued urban expansion in Ahmedabad was associated with increasingly heterogeneous urban thermal conditions and changing vegetation-temperature relationships across the metropolitan region, highlighting the importance of ecological continuity and spatial vegetation distribution in climate-sensitive urban planning within rapidly urbanising semi-arid cities.

Keywords: Urban Heat Island; Land Surface Temperature; Ahmedabad; Remote Sensing; Google Earth Engine; NDVI; NDBI; Urban Expansion; Urban Thermal Heterogeneity; Semi-arid Cities.

1. Introduction

Rapid urbanization has significantly altered land-cover patterns across cities worldwide, contributing to rising land surface temperatures (LST) and intensified urban heat island (UHI) effects (Alcoforado and Andrade, 2008; Oke, 1982; Voogt and Oke, 2003). The replacement of vegetated and permeable surfaces with impervious materials such as concrete and asphalt alters surface energy exchange, reduces evapotranspiration, and increases heat storage within urban environments (Kayet et al., 2016; Weng et al., 2004; Yuan and Bauer, 2007). Foundational urban climate research established that these thermal changes are closely linked to urban morphology, surface composition, and energy balance processes (Oke, 1982; Voogt and Oke, 2003). Recent studies further show that urban thermal behavior is strongly influenced by spatial heterogeneity in land cover and built-up structure, particularly within rapidly expanding metropolitan regions (Hernández-Herráez et al., 2025; Wan et al., 2026; Wu et al., 2026). In semi-arid cities, where vegetation cover is often limited and summer temperatures remain persistently high, continued impervious expansion can further intensify urban thermal stress and reduce the cooling influence of vegetated surfaces (Gholamian Moghaddam et al., 2025; Wang et al., 2018).

Remote sensing has become one of the most widely used approaches for examining urban thermal environments because it enables consistent long-term observation of land surface processes across large spatial scales (Gorelick et al., 2017; Voogt and Oke, 2003). Thermal infrared satellite data allow retrieval of land surface temperature, while spectral indices such as the Normalised Difference Vegetation Index (NDVI) and Normalised Difference Built-up Index (NDBI) provide useful measures of vegetation cover and urban expansion (McFEETERS, 1996; Rouse et al., 1974; Zha et al., 2003). Previous studies have consistently reported negative relationships between vegetation cover and LST, indicating that vegetated areas contribute to localised cooling through shading and evapotranspirative processes, whereas dense built-up surfaces are generally associated with higher surface temperatures (Wang et al., 2018; Weng et al., 2004; Yuan and Bauer, 2007; Zhang et al., 2026). Cloud-based geospatial platforms such as Google Earth Engine have further expanded the use of long-term remote sensing datasets in urban climate research (Gorelick et al., 2017; Stamou and Stylianidis, 2025). Recent studies using Google Earth Engine and Landsat datasets have demonstrated the value of these approaches for examining urban heat island dynamics, land-cover change, and thermal variability within rapidly urbanising cities (Roy and Bari, 2022; Sharma et al., 2025; Singh et al., 2024).

In India, rapid metropolitan expansion has intensified urban heat island effects across several major cities, particularly in regions undergoing extensive land-cover transformation and infrastructure growth (Islam et al., 2024; Mandal and Chanda, 2025; Manna et al., 2026). Ahmedabad, one of western India's fastest-growing metropolitan regions, has experienced

substantial urban expansion over the past two decades under conditions of high summer temperatures and a semi-arid climate (Gupta et al., 2024; Joshi et al., 2015; Mohammad et al., 2019). These characteristics make the city especially vulnerable to persistent surface warming and heatwave-related thermal stress (Azhar et al., 2014). Previous studies conducted in Ahmedabad have reported strong associations between built-up concentration and elevated land surface temperature, while vegetated and peripheral areas generally exhibit lower surface temperatures (Gupta, 2025; Joshi et al., 2015; Mohammad et al., 2019). More recent urban climate research has emphasised the importance of spatial heterogeneity in shaping intra-urban thermal patterns, demonstrating that localised land-cover composition, vegetation fragmentation, and urban morphology can produce substantial variation in thermal conditions within the same metropolitan region (Chen et al., 2022; Hernández-Herráez et al., 2025; Ramachandra et al., 2025; Wu et al., 2026).

Beyond regional case studies, recent urban climate research has increasingly emphasised the importance of spatial and socio-environmental heterogeneity in shaping urban thermal patterns within rapidly expanding metropolitan regions (Ramsay et al., 2023). Studies increasingly suggest that thermal variability within cities is shaped not only by land-cover conversion, but also by vegetation configuration, built-up concentration, and localised urban morphology (Hernández-Herráez et al., 2025; Wu et al., 2026). Despite these advances, many existing studies remain limited by short temporal coverage, single-period analyses, or insufficient integration of land surface temperature, vegetation dynamics, and built-up expansion across longer temporal scales. This limitation is particularly evident in rapidly urbanising semi-arid cities such as Ahmedabad, where sustained urban growth, fragmented vegetation cover, and persistent summer heat create increasingly heterogeneous thermal conditions. Comprehensive multi-decadal assessments examining how urban expansion has altered the spatial relationship between vegetation cover, built-up intensity, and surface thermal behavior remain comparatively limited.

Therefore, this study examines long-term changes in land surface temperature, vegetation cover, and built-up expansion in Ahmedabad between 2000 and 2025 using multi-temporal Landsat data at five-year intervals. The study investigates how urban growth relates to changes in the spatial relationship between vegetation cover, built-up intensity, and urban thermal patterns within the city. Specifically, the objectives are to: (i) characterize the spatiotemporal evolution of land surface temperature across Ahmedabad between 2000 and 2025; (ii) evaluate temporal changes in vegetation dynamics using the Normalised Difference Vegetation Index (NDVI); (iii) analyze spatiotemporal variation in relative built-up intensity using standardised NDBI (NDBIz); and (iv) examine how vegetation dynamics and built-up intensity were associated with urban thermal variability across the study period.

2. Study Area

Figure 1. Study area showing the spatial extent of Ahmedabad Municipal Corporation (AMC), India, used for analysis of land surface temperature (LST), vegetation dynamics (NDVI), and urban expansion. Boundary data: OpenCity (2024). Basemap © OpenStreetMap contributors, © CARTO.

Ahmedabad, located in the state of Gujarat in western India, is one of the fastest-growing metropolitan regions in the country and represents a semi-arid urban environment undergoing rapid spatial transformation (Gupta, 2025; Mohammad et al., 2019). The city is situated along the Sabarmati River between approximately 23.02°N–23.03°N latitude and 72.35°E–72.58°E longitude at an elevation of approximately 55 m above sea level (Manorama Mohanty et al., 2022). The study area includes the Ahmedabad Municipal Corporation (AMC) region along with its expanding peri-urban fringe, where substantial land-use transitions have occurred over the past two decades.

Ahmedabad experiences a hot semi-arid climate characterised by intense summer heat, highly seasonal rainfall, and prolonged dry periods. Average annual rainfall is approximately 824 mm, with most precipitation concentrated during the southwest monsoon season. Weather conditions remain extremely hot and dry

between March and June, with maximum temperatures frequently exceeding 40°C during the pre-monsoon period (Manorama Mohanty et al., 2022). These climatic conditions, combined with limited vegetation cover and high solar exposure, increase the city's sensitivity to surface warming and urban heat island formation (Oke, 1982; Voogt and Oke, 2003; Azhar et al., 2014).

Urban growth in Ahmedabad has been spatially uneven, with rapid expansion of built-up areas into formerly agricultural and open landscapes, particularly along the urban periphery. Expansion of impervious surfaces has altered the spatial distribution of vegetation and intensified land-cover contrasts across the metropolitan region. Previous studies in Ahmedabad have reported strong associations between built-up concentration and elevated land surface temperature, while vegetated and peri-urban areas generally exhibit comparatively lower surface temperatures (Gupta, 2025; Joshi et al., 2015; Mohammad et al., 2019).

The coexistence of dense urban cores, transitional peri-urban environments, river-associated landscapes, and fragmented vegetation creates a heterogeneous urban landscape well suited for examining spatial variation in vegetation cover, built-up intensity, and thermal behavior. Ahmedabad therefore provides an important setting for investigating how long-term urban expansion is associated with urban thermal patterns and vegetation–temperature relationships within a rapidly growing semi-arid city.

3. Methodology

This study employs multi-temporal, multi-sensor Landsat satellite data to analyze the ecological impacts of urban expansion on land surface temperature (LST) and vegetation dynamics in Ahmedabad from 2000 to 2025. The methodology uses spectral indices and thermal retrieval methods to examine long-term changes in urban thermal and vegetation patterns.

3.1 Data Sources

Multi-temporal, multi-sensor Landsat imagery was acquired from the United States Geological Survey (USGS) Landsat Collection 2 Level 2 archive (United States Geological Survey, 2020) through the Google Earth Engine (GEE) cloud computing platform (Gorelick et al., 2017). Six temporal snapshots at approximately five-year intervals between 2000 and 2025 were analysed to examine long-term changes in land surface temperature, vegetation cover, and built-up intensity across Ahmedabad, India.

Imagery from multiple Landsat sensor generations was used to maintain temporal continuity throughout the study period. The datasets included Landsat 5 Thematic Mapper (TM), Landsat 7 Enhanced Thematic Mapper Plus (ETM+), Landsat 8 Operational Land Imager/Thermal Infrared Sensor (OLI/TIRS), and Landsat 9 Operational Land Imager-2/Thermal Infrared Sensor-2 (OLI-2/TIRS-2). All imagery was obtained from atmospherically corrected Collection 2 Level 2 products,

which provide calibrated surface reflectance and surface temperature data (United States Geological Survey, 2020).

The temporal intervals analysed were:

- 2000 → Landsat 5 TM
- 2005 → Landsat 7 ETM+
- 2010 → Landsat 5 TM
- 2015 → Landsat 8 OLI/TIRS
- 2020 → Landsat 8 OLI/TIRS
- 2025 → Landsat 9 OLI-2/TIRS-2

To maintain seasonal consistency, imagery was restricted to the pre-monsoon summer period (May–June) for all study years. This period corresponds with peak surface heating conditions in Ahmedabad while reducing seasonal variability associated with vegetation and surface moisture. Similar seasonal selection approaches have been adopted in previous urban thermal studies conducted in semi-arid and tropical urban environments (Mohammad et al., 2019; Weng et al., 2004).

The study area comprised the Ahmedabad Municipal Corporation (AMC) administrative boundary in Gujarat, India. The boundary polygon was imported into Google Earth Engine as a FeatureCollection asset and used for spatial filtering, masking, clipping, and sampling operations. All analyses were conducted at 30 m spatial resolution, and exported raster products were generated in the EPSG:4326 geographic coordinate system for subsequent GIS and statistical analysis.

3.2 Google Earth Engine Preprocessing

All preprocessing and raster derivation workflows were conducted within the Google Earth Engine cloud-computing environment (Gorelick et al., 2017). Preprocessing was carried out to ensure temporal consistency across multiple Landsat sensor generations while reducing atmospheric contamination, cloud-related artefacts, and inter-sensor variability.

3.2.1 Cloud Masking and quality filtering

Clouds, cloud shadows, and related atmospheric artefacts were removed using the QA_PIXEL quality assurance band available within Landsat Collection 2 Level 2 products (United States Geological Survey, 2020). Bitwise masking was applied to exclude pixels affected by cloud contamination and cloud shadows.

The following QA_PIXEL bits were masked:

- Bit 3 → cloud shadow
- Bit 4 → snow/cloud contamination
- Bit 5 → clouds

Pixels flagged within these categories were excluded from all analyses.

To further reduce atmospheric contamination, image collections were filtered using scene-level cloud cover metadata. Due to differences in image availability between sensor generations, separate cloud cover thresholds were applied:

- Landsat 5 TM / Landsat 7 ETM+ → CLOUD_COVER < 50%.
- Landsat 8 OLI/TIRS / Landsat 9 OLI-2/TIRS-2 → CLOUD_COVER < 20%.

The comparatively relaxed threshold for earlier Landsat sensors was necessary to maintain sufficient image availability during the selected summer acquisition period.

3.2.2. Temporal compositing and reflectance scaling

Median compositing was applied to yearly image collections to generate representative seasonal surface conditions while reducing residual cloud contamination, sensor noise, and anomalous observations. Median composites were selected instead of mean composites because they are less sensitive to outlier pixels and remaining atmospheric artefacts.

Surface reflectance bands were scaled using the USGS Collection 2 Level 2 scaling equation (United States Geological Survey, 2020):

\text{Reflectance} = (DN \times 0.0000275) - 0.2

This scaling procedure was applied consistently across all Landsat sensor generations to maintain radiometric comparability throughout the study period. All derived raster products were subsequently clipped to the Ahmedabad Municipal Corporation (AMC) boundary to ensure spatial consistency across years and variables.

3.2.3 Cross-sensor harmonization and workflow refinement

During preliminary analysis, inconsistencies were observed in interannual comparisons of raw NDBI values, particularly between Landsat 5 TM and Landsat 8/9 OLI sensors. In contrast to NDVI and LST products, raw NDBI distributions exhibited sensor-dependent shifts that affected temporal comparability of built-up intensity patterns. To improve interannual consistency across the multi-sensor dataset, several workflow refinements were implemented, including the use of consistent May–June acquisition windows, sensor-consistent spectral band selection for index calculation, fixed visualization ranges for NDVI and LST products, and standardised preprocessing procedures across all study years. Additional harmonization and standardization procedures applied to NDBI products are described in Section 3.5.

3.3 Land Surface Temperature (LST)

Land Surface Temperature (LST) was derived directly from Landsat Collection 2 Level 2 Surface Temperature products available within Google Earth Engine. These products provide atmospherically corrected surface temperature estimates generated using radiative transfer algorithms and sensor-specific calibration coefficients supplied by the United States Geological Survey(United States Geological Survey, 2020). Use of Collection 2 Level 2 products ensured methodological consistency across multiple Landsat sensor generations and

improved reliability in long-term temporal comparison.

Thermal infrared bands used for LST retrieval varied according to Landsat sensor generation:

- Landsat 5 TM → ST_B6
- Landsat 7 ETM+ → ST_B6
- Landsat 8 OLI/TIRS → ST_B10
- Landsat 9 OLI-2/TIRS-2 → ST_B10

Scaled Landsat Collection 2 Level 2 surface temperature values were converted to temperature in Kelvin using the USGS-recommended scaling equation (United States Geological Survey, 2020):

$$LST\ (K)\ =\ (DN\ \times\ 0.00341802)\ +\ 149$$

Kelvin temperatures were subsequently converted to degrees Celsius using:

$$LST(°C)\ =\ LST\ (K)\ -\ 273.15$$

The present study used atmospherically corrected Landsat Collection 2 Level 2 Surface Temperature products directly within Google Earth Engine. Consequently, additional emissivity correction or independent radiative transfer modelling was not implemented. Standardised Collection 2 surface temperature products have been widely used in recent urban thermal studies because of their radiometric consistency and suitability for long-term environmental analysis (Hurduc et al., 2024; United States Geological Survey, 2020).

Invalid pixels and masked regions were excluded prior to analysis to improve spatial consistency and reduce anomalous observations. Final LST rasters were clipped to the Ahmedabad Municipal Corporation (AMC) boundary and exported at 30 m spatial resolution for subsequent spatial visualization and statistical analysis.

Within the present study, LST was used to evaluate spatial and temporal variation in urban surface thermal conditions across Ahmedabad. Spatial and temporal variations in LST were subsequently examined in relation to vegetation cover and built-up intensity, alongside supplementary assessment of NDWI-derived moisture-related variability between 2000 and 2025.

3.4 Spectral Indices

Three spectral indices were derived from Landsat surface reflectance products to evaluate vegetation cover, built-up intensity, and surface moisture conditions across Ahmedabad: the Normalised Difference Vegetation Index (NDVI), the Normalised Difference Water Index (NDWI), and the Normalised Difference Built-up Index (NDBI). All indices were calculated using atmospherically corrected surface reflectance bands obtained from Landsat Collection 2 Level 2 datasets.

3.4.1 Normalised Difference Vegetation Index (NDVI)

Vegetation cover and vegetation-related thermal associations were assessed using the Normalised Difference Vegetation Index (NDVI) (Rouse et al., 1974):

$$NDVI\ =\ \frac{NIR-Red}{NIR+Red}$$

For Landsat 5 TM and Landsat 7 ETM+ imagery, the following bands were used:

- Near Infrared (NIR) → SR_B4
- Red → SR_B3

For Landsat 8 OLI/TIRS and Landsat 9 OLI-2/TIRS-2 imagery:

- Near Infrared (NIR) → SR_B5
- Red → SR_B4

NDVI values theoretically range from −1 to +1, with higher values indicating denser and healthier vegetation cover. Within the present study, NDVI was interpreted as a proxy for vegetation-mediated ecosystem functions associated with evapotranspiration, shading, and microclimatic cooling. Previous studies have consistently indicated strong negative relationships between NDVI and urban land surface temperature, highlighting the role of vegetation in moderating urban heat island effects (Weng et al., 2004; Yuan and Bauer, 2007).

3.4.2 Normalised Difference Water Index (NDWI)

Surface moisture conditions were evaluated using the Normalised Difference Water Index (NDWI) (McFEETERS, 1996):

$$NDWI = \frac{Green - NIR}{Green + NIR}$$

For Landsat 5 TM and Landsat 7 ETM+ imagery:

- Green → SR_B2
- NIR → SR_B4

For Landsat 8 OLI/TIRS and Landsat 9 OLI-2/TIRS-2 imagery:

- Green → SR_B3
- NIR → SR_B5

NDWI was used to identify moisture-rich and water-associated surfaces across the study area. Moisture availability is associated with surface energy partitioning and evapotranspiration processes, both of which affect localised thermal conditions within urban environments (Weng et al., 2004).

3.4.3 Normalised Difference Built-up Index (NDBI)

Built-up intensity was assessed using the Normalised Difference Built-up Index (NDBI) (Zha et al., 2003):

$$NDBI = \frac{SWIR - NIR}{SWIR + NIR}$$

For Landsat 5 TM and Landsat 7 ETM+ imagery:

- Shortwave Infrared (SWIR1) → SR_B5
- Near Infrared (NIR) → SR_B4

For Landsat 8 OLI/TIRS and Landsat 9 OLI-2/TIRS-2 imagery:

- Shortwave Infrared (SWIR1) → SR_B6
- Near Infrared (NIR) → SR_B5

Higher NDBI values generally correspond to built-up and impervious surfaces, whereas lower values are typically associated with vegetation and water-covered areas. In the

present study, NDBI was used to represent relative built-up intensity and impervious surface concentration associated with urban expansion.

Previous urban thermal studies have reported strong positive relationships between NDBI and land surface temperature, indicating that impervious surfaces contribute substantially to urban thermal amplification through reduced evapotranspiration and increased heat storage (Mohammad et al., 2019; Yuan and Bauer, 2007).

3.5 Cross-sensor Harmonisation and Standardisation Framework

Interannual comparison of raw NDBI values revealed noticeable distributional differences among Landsat sensor generations, particularly between Landsat 5 TM/7 ETM+ and Landsat 8/9 OLI datasets. Unlike NDVI and LST products, which remained comparatively stable under consistent visualization and preprocessing conditions, raw NDBI values exhibited sensor-related shifts that complicated direct temporal comparison of built-up intensity patterns. Similar inter-sensor variability has been reported in previous multi-temporal Landsat urban studies (Liyaqat et al., 2025; Roy and Bari, 2022; Singh et al., 2024).

To reduce sensor-related variability and improve interannual consistency, NDBI values were standardised independently for each study year using z-score normalization. The standardised built-up intensity index (NDBIz) was calculated as:

$$NDBI_Z = \frac{NDBI - \mu_{year}}{\sigma_{year}}$$

where:

- μ_{year} represents the mean NDBI value for a given year, and
- σ_{year} represents the corresponding standard deviation.

Year-wise normalization was adopted because Landsat sensor generations differ in radiometric response and spectral sensitivity within the SWIR and NIR wavelengths used for NDBI calculation. Standardization reduced artificial interannual variability associated with sensor differences while preserving relative spatial contrasts in built-up intensity within each year. Consequently, NDBIz was interpreted as a measure of relative built-up intensity rather than absolute spectral magnitude.

Additional harmonization procedures were applied throughout the workflow to maintain temporal consistency across the multi-sensor dataset. These included restricting all imagery to May–June acquisition periods, maintaining consistent spectral band selection across Landsat sensors, applying uniform preprocessing procedures, and generating all raster products using identical clipping and masking operations. Together, these procedures improved the reliability of long-term comparison of urban expansion patterns across Ahmedabad.

3.6 Data extraction & Sampling

Pixel-based sampling was conducted within Google Earth Engine to support statistical

analysis of relationships between land surface temperature, vegetation cover, moisture conditions, and built-up intensity across Ahmedabad.

For each study year, raster layers representing:

- Land Surface Temperature (LST),
- Normalised Difference Vegetation Index (NDVI),
- Normalised Difference Water Index (NDWI),
- and standardised built-up intensity (NDBIz)

were combined into a multiband raster stack prior to sampling. This ensured that sampled observations represented spatially corresponding pixel values across all variables.

Random sampling was performed at 30 m spatial resolution using 5000 spatially distributed pixels per year. The sampling framework was intended to reduce spatial bias while capturing a range of urban landscape conditions, including dense built-up areas, vegetated surfaces, peri-urban zones, and moisture-associated regions.

Sampled pixel values were exported from Google Earth Engine as comma-separated value (CSV) files. Separate yearly datasets were subsequently merged in R to produce a unified multi-temporal dataset for statistical analysis and temporal comparison.

The final dataset represented a pixel-level environmental database integrating thermal, vegetation, moisture, and built-up characteristics across all study years. This dataset was used for correlation analysis, regression modelling, and temporal comparison of urban thermal patterns between 2000 and 2025.

3.7 Statistical Analysis

All statistical analyses were conducted in R to evaluate relationships between land surface temperature (LST), vegetation cover, built-up intensity, and surface moisture conditions across Ahmedabad between 2000 and 2025. Separate yearly datasets exported from Google Earth Engine were merged into a unified multi-temporal dataset containing pixel-level observations for all environmental variables and study years.

3.7.1 Descriptive Statistics and Temporal Trends

Descriptive statistics were calculated to characterize the distribution and temporal variation of environmental variables across the study area. Summary measures included mean, median, minimum, maximum, and standard deviation.

Temporal summaries were generated separately for each study year for:

- land surface temperature (LST),
- vegetation cover (NDVI),
- built-up intensity (NDBIz),
- and surface moisture conditions (NDWI).

These statistics were used to examine long-term variation in thermal conditions, vegetation cover, moisture patterns, and

built-up intensity across Ahmedabad prior to correlation and regression analysis.

3.7.2 Correlation Analysis

Pearson correlation analysis was conducted to quantify relationships between land surface temperature (LST) and the environmental variables NDVI, NDWI, and NDBIz.

The Pearson correlation coefficient was calculated as:

$$r = \frac{cov\,(X,Y)}{\sigma_x \sigma_y}$$

where:

- cov(X,Y) represents covariance between paired variables, and
- σ represents standard deviation.

Correlation analysis was performed across the complete multi-temporal dataset and separately for each study year. This enabled comparison of overall environmental relationships as well as temporal variation in thermal controls across the study period. Statistical significance was assessed using two-tailed tests, with $p < 0.05$ considered statistically significant.

3.7.3 Regression Modelling Framework

Multiple linear regression models were developed to evaluate the association of vegetation cover, built-up intensity, surface moisture conditions, and temporal variation on land surface temperature across Ahmedabad.

The general model structure was:

$$LST = \beta_o + \beta_1 (NDVI) + \beta_2 (NDBI_Z) + \beta_3 (NDWI) + \beta_4 (Year) + \varepsilon$$

where:

- β_0 represents the intercept,
- $\beta_{1\text{-}4}$ represents regression coefficients, and
- ε represents residual error.

A progressive modelling framework was used to compare explanatory performance across different model structures. The modelling sequence included simple bivariate models, multivariate environmental models, and temporally adjusted models incorporating year effects.

Year was treated as a categorical factor variable using dummy-variable encoding, with 2000 used as the reference year. The final regression model included NDVI, NDWI, $NDBI_z$, and year-specific effects.

The final multivariate model demonstrated the strongest explanatory performance and was used to evaluate long-term urban thermal variability across Ahmedabad.

3.7.4 Model Comparison and Standardised Coefficients

Competing regression models were evaluated using adjusted R^2, Akaike Information Criterion (AIC), residual diagnostics, and coefficient interpretability. Adjusted R^2 was used to assess explanatory performance while accounting for model complexity, whereas lower AIC values were interpreted as indicating improved model fit relative to competing specifications.

To compare the relative association of predictor variables measured on different scales, standardised beta coefficients were calculated using z-score standardised variables. Standardised coefficients enabled comparison of the relative association of vegetation cover, built-up intensity, and surface moisture conditions on land surface temperature.

3.7.5 Multicollinearity and Diagnostic Testing

Variance Inflation Factor (VIF) analysis was conducted to evaluate multicollinearity among predictor variables. Elevated VIF values were observed for NDVI and NDWI due to their strong covariance across the study area. However, both variables were retained because they represent distinct ecological dimensions related to vegetation cover and surface moisture conditions, and model coefficients remained stable across alternative specifications.

Regression assumptions were evaluated using residual versus fitted plots, Q–Q plots, scale–location plots, and residual leverage analysis. These diagnostics were used to assess linearity, residual normality, homoscedasticity, and influential observations.

Minor heteroskedasticity and residual tail deviations were observed in some model outputs. However, the large sample size and stability of regression coefficients supported the overall robustness of the final regression models.

3.7.6 Temporal Variation in Urban Thermal Relationships

To evaluate how environmental controls on urban temperature changed through time, separate yearly regression models were developed for each study year.

Temporal comparison focused on variation in NDVI–LST relationships, NDBIz-LST association, and changes in regression coefficient structure across the study period. Regression coefficients derived from yearly models were compared to examine long-term variation in urban thermal patterns associated with urban expansion and land-cover transformation.

Particular attention was given to how vegetation–temperature relationships varied under increasing built-up intensity and changing urban landscape composition. This framework enabled interpretation of temporal variation in spatial relationships between vegetation cover, built-up intensity, and urban thermal conditions across Ahmedabad.

3.8 Software and Visualisation

All remote sensing preprocessing, raster derivation, and spatial sampling workflows were conducted using Google Earth Engine (Gorelick et al., 2017). Statistical analyses were performed in R using packages including tidyverse, ggplot2, car, broom, GGally, viridis, and ggpmisc.

Spatial visualization, cartographic layout preparation, and final map composition were conducted in QGIS. Statistical figures were generated in R, while map layouts and spatial visualizations were prepared using GIS-based cartographic workflows.

All figures and tables presented in the study were derived directly from the processed datasets and statistical outputs generated through the analytical framework described above.

4. Results

4.1 Spatiotemporal Evolution of Urban Thermal and Ecological Patterns

Multi-temporal analysis of land surface temperature (LST), vegetation cover (NDVI), and built-up intensity (NDBIz) revealed pronounced spatial changes across Ahmedabad between 2000 and 2025 (Figure 2). The maps show progressive urban expansion alongside shifts in vegetation distribution and surface thermal patterns across the metropolitan region.

The LST maps indicate gradual expansion and intensification of urban thermal hotspots over the study period. In 2000, elevated surface temperatures were relatively localised within parts of the historical urban core and isolated built-up clusters. By 2010, high-temperature zones had become more spatially continuous across densely urbanised sectors, particularly within central and eastern Ahmedabad. In 2025, thermal patterns appeared more heterogeneous, although elevated LST values remained widespread across major urbanised areas. Lower surface temperatures were consistently associated with the Sabarmati River corridor and vegetated peripheral regions.

NDVI patterns exhibited uneven temporal change across the metropolitan region. Earlier years (2000–2010) showed fragmented vegetation distribution across much of the urban landscape. In later years, particularly 2020 and 2025, localised increases in vegetation cover became more visible within western Ahmedabad, peri-river landscapes, and peripheral sectors. However, densely urbanised central and eastern corridors continued to exhibit relatively sparse vegetation cover and limited continuity of green spaces.

The NDBIz maps indicate substantial expansion of built-up intensity across Ahmedabad over time. Increasing built-up concentration was most evident within eastern, southeastern, and central sectors, where open and transitional landscapes were progressively converted into impervious urban surfaces.

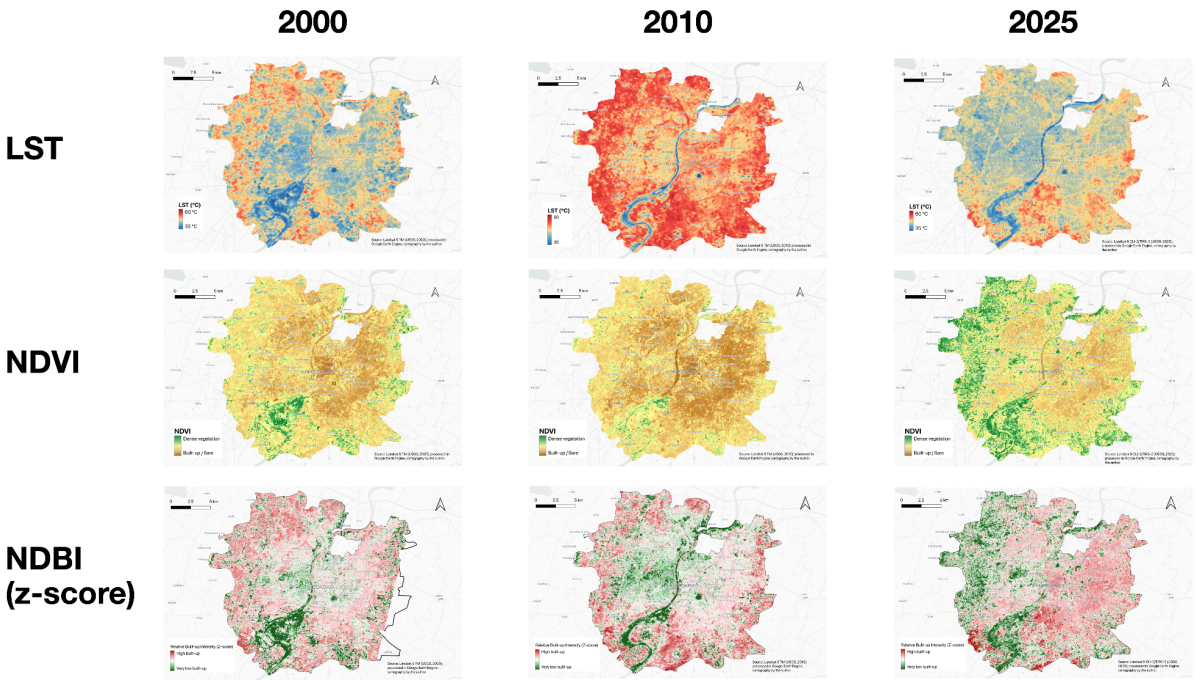

Figure 2. Spatiotemporal evolution of land surface temperature (LST), vegetation cover (NDVI), and standardised built-up intensity (NDBIz) across Ahmedabad between 2000 and 2025. Representative maps from 2000, 2010, and 2025 are shown to illustrate major spatial changes in thermal conditions, vegetation distribution, and urban expansion. Full multi-temporal map series for all study years are provided in Supplementary Figure S1-S3.

In contrast, parts of western Ahmedabad retained comparatively lower relative built-up intensity despite continued urban development, indicating spatial variation in urban form and land-cover composition across the metropolitan region.

Spatial correspondence between elevated NDBIz values and intensified LST patterns suggests a strong association between built-up expansion and urban thermal amplification. Areas with comparatively greater vegetation continuity generally exhibited lower thermal intensity. Overall, the spatial analysis indicates increasing intra-urban heterogeneity in thermal conditions, vegetation distribution, and built-up intensity across Ahmedabad between 2000 and 2025.

4.2 Temporal Trends in LST, Vegetation Cover, and Built-up Intensity

Descriptive statistical summaries were calculated for land surface temperature (LST), vegetation cover (NDVI), standardised built-up intensity (NDBIz), and

surface moisture conditions (NDWI) across all study years to evaluate temporal changes in Ahmedabad's urban environment between 2000 and 2025 (Table 1).

Because NDBI values were standardised independently for each year using z-score normalization, annual mean NDBIz values remained centered near zero and primarily reflect relative spatial variability in built-up intensity rather than absolute spectral magnitude. Temporal interpretation of urban expansion therefore relied mainly on spatial distribution patterns and regression relationships rather than direct comparison of yearly mean NDBIz values.

Year	Mean LST (°C)	Mean NDVI	Mean NDBIz	Mean NDWI
2000	46.11	0.223	-0.009	-0.301
2005	49.54	0.205	0.023	-0.306
2010	49.78	0.182	0.003	-0.25
2015	48.88	0.247	0.011	-0.316
2020	51.6	0.248	0.002	-0.319
2025	44.26	0.301	-0.007	-0.343

Table 1. Summary statistics of land surface temperature (LST), vegetation cover (NDVI), standardised built-up intensity (NDBIz), and surface moisture conditions (NDWI) across Ahmedabad between 2000 and 2025.

Mean land surface temperature showed considerable temporal variability during the study period, increasing from 46.11°C in 2000 to 49.78°C in 2010 and reaching a peak of 51.60°C in 2020 before declining to 44.26°C in 2025 (Table 1). The largest increase in mean LST occurred between 2000 and 2020, consistent with the expansion of high-temperature zones identified in the spatial analysis.

Mean NDVI declined from 0.223 in 2000 to 0.182 in 2010, indicating reduction and fragmentation of vegetation cover during periods of accelerated urban growth. In later years, NDVI values increased progressively, reaching 0.247 in 2015, 0.248 in 2020, and 0.301 in 2025. Despite this increase, vegetation distribution remained uneven across the metropolitan region.

Mean NDWI values remained consistently negative throughout the study period, ranging from −0.250 to −0.343, indicating generally limited surface moisture conditions across Ahmedabad. Interannual variation in NDWI was comparatively minor relative to the stronger temporal variability observed in LST and NDVI.

Although annual mean NDBIz values remained close to zero due to year-wise standardization, spatial analysis indicated continued expansion of built-up intensity across central, eastern, and southeastern sectors of Ahmedabad over time. In contrast, parts of western Ahmedabad retained

comparatively lower relative built-up intensity despite continued urban development.

Overall, the temporal trends align closely with the spatial patterns shown in Figure 2 and indicate substantial changes in Ahmedabad's thermal conditions, vegetation distribution, and built-up expansion between 2000 and 2025.

4.3 Environmental Relationships and Thermal Controls

Relationships between vegetation cover, built-up intensity,, and land surface temperature varied across Ahmedabad between 2000 and 2025. These dynamics were examined using temporal trends in vegetation greenness, NDVI–LST relationship strength, and built-up thermal association alongside correlation analysis and yearly NDVI–LST regression relationships (Figures 3–5).

Figure 3 shows the temporal evolution of mean NDVI, NDVI–LST relationship strength, and built-up association across the study period. Mean NDVI values declined between 2000 and 2010 before increasing progressively after 2015, reaching their highest levels in 2025. In contrast, NDVI–LST relationship strength, represented by standardised yearly NDVI regression coefficients, followed a different trajectory. Stronger negative NDVI–LST relationships were observed during 2000 and 2005, whereas these relationships became progressively weaker after 2010.

At the same time, built-up thermal relationship strength increased through time. Standardised NDBIz regression coefficients indicate progressively stronger positive relationships between built-up intensity and land surface temperature, especially after 2010. Although intermediate fluctuations were present, the overall pattern suggests increasing thermal intensity associated with expanding impervious surfaces.

The correlation matrix further illustrates relationships among the analysed environmental variables (Figure 4).

NDVI exhibited a moderate negative correlation with LST ($r = -0.29$), whereas NDBIz showed a moderate positive relationship with LST ($r = 0.51$).

NDWI remained weakly correlated with LST ($r = 0.12$) while exhibiting a strong negative correlation with NDVI ($r = -0.96$), indicating substantial covariance between vegetation and surface moisture conditions within the study area.

Yearly NDVI–LST relationships were further examined using density-based regression visualization (Figure 5).

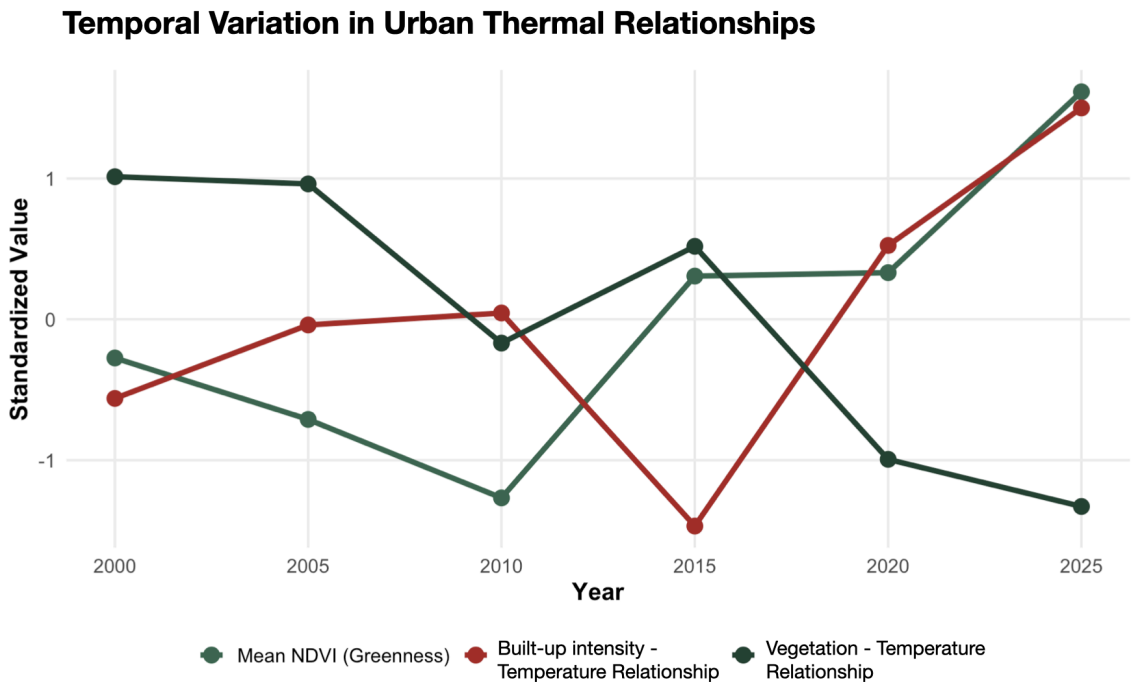

Figure 3. Temporal variation in mean NDVI, strength of NDVI–LST relationships, and standardised NDBIz–LST relationship coefficients across Ahmedabad between 2000 and 2025.

Across all study years, NDVI maintained a generally negative relationship with land surface temperature, although the strength and structure of this relationship varied between years. In 2000, the NDVI–LST relationship exhibited a comparatively steep negative slope, indicating stronger negative NDVI–LST relationships associated with vegetated surfaces. By 2010, the regression slope became noticeably flatter, while the density distribution shifted toward higher temperature concentrations despite moderate vegetation presence. In 2025, NDVI values were generally higher than those observed during earlier years; however, the negative NDVI–LST relationship remained weaker relative to 2000, with broader thermal dispersion across similar NDVI ranges. The density structure of the NDVI–LST relationships also became more heterogeneous over time. Earlier years exhibited clearer thermal differentiation across vegetation conditions, whereas later years showed greater temperature variability within comparable NDVI ranges (Figure 5). Overall, the environmental relationships indicate increasing variability in Ahmedabad's urban thermal conditions under continued urban expansion, with vegetation cover and built-up intensity exhibiting differing associations with land surface temperature across the study period.

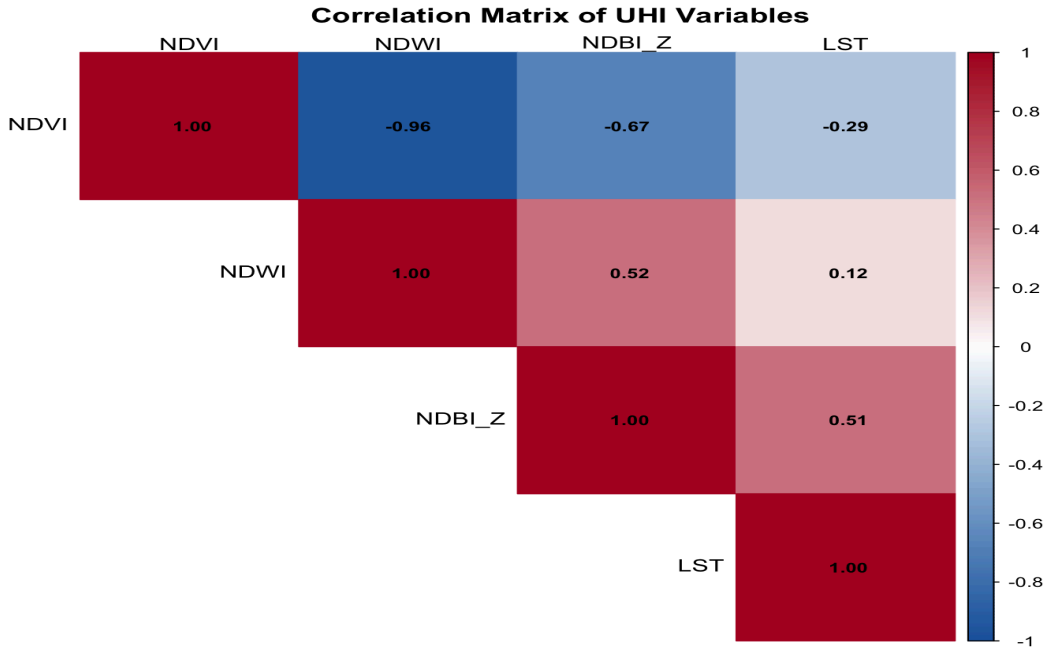

Figure 4. Pearson correlation matrix showing relationships among vegetation cover (NDVI), surface moisture conditions (NDWI), standardised built-up intensity (NDBIz), and land surface temperature (LST) across Ahmedabad between 2000 and 2025.

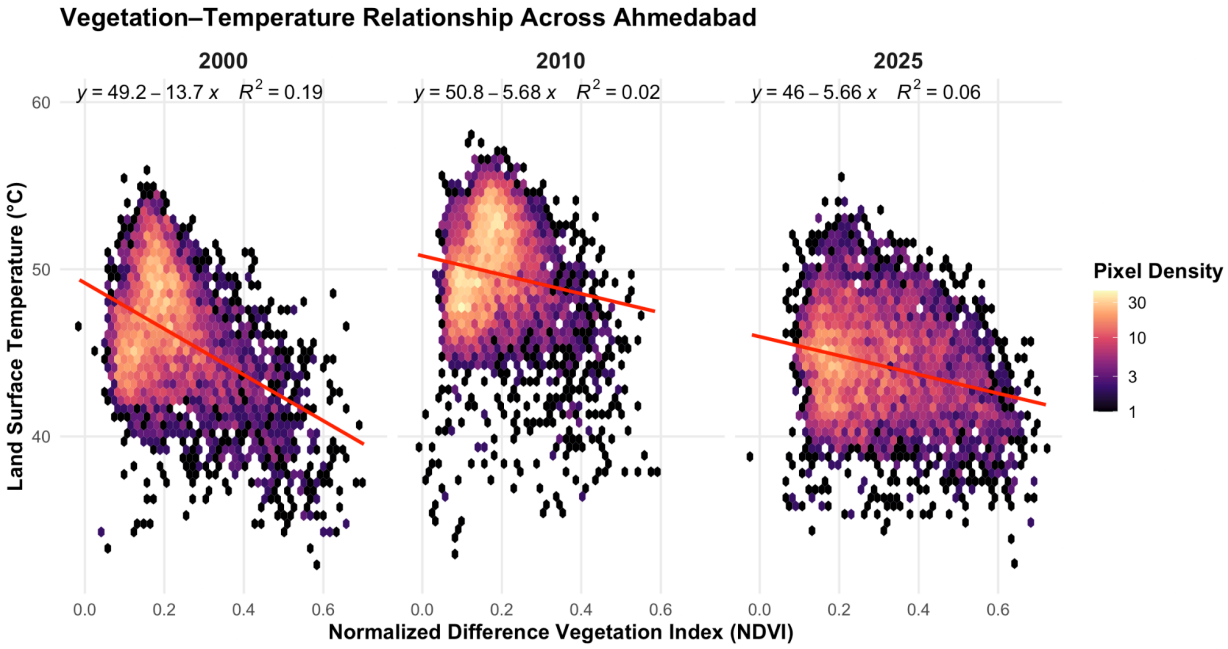

Figure 5. Density-based regression relationships between vegetation cover (NDVI) and land surface temperature (LST) across Ahmedabad for 2000, 2010, and 2025. Regression trends and pixel-density distributions illustrate temporal variation in NDVI–LST relationships across the study period.

4.4 Regression Modelling of Urban Thermal Controls

Multiple regression models were developed to evaluate the combined association of vegetation cover (NDVI), built-up intensity (NDBIz), surface moisture conditions (NDWI), and temporal variation on land surface temperature across Ahmedabad. Model comparison statistics are presented in Table 2.

Regression model performance improved progressively as additional environmental and temporal variables were incorporated into the modelling framework. Model 1, which included NDVI alone, showed relatively limited explanatory capacity (Adjusted $R^2 = 0.086$). Inclusion of NDBIz and NDWI in Model 2 increased the adjusted R^2 to 0.405 while reducing residual error and AIC values, indicating improved representation of urban thermal variability.

Model	Predictors	Adjusted R^2	Residual SE	AIC
Model 1	NDVI	0.086	3.966	166845.7
Model 2	NDVI, NDBIz, NDWI	0.405	3.198	154012.7
Model 3	NDVI, NDBIz, NDWI, Year	0.69	2.311	134639.2

Table 2. Comparison of regression model performance for predicting land surface temperature (LST) across Ahmedabad using environmental and temporal predictors. Model performance improved with the inclusion of built-up intensity, NDWI, and temporal effects, with Model 3 showing the highest explanatory capacity.

The strongest performance was observed in Model 3, which incorporated temporal effects alongside environmental predictors. Model 3 produced the highest adjusted R^2 value (0.690) and the lowest residual standard error and AIC values among all tested models, indicating that temporal variation contributed substantially to explaining differences in Ahmedabad's urban thermal conditions between 2000 and 2025.

Standardised beta coefficients derived from Model 3 are presented in Figure 6. NDWI exhibited the largest negative standardised coefficient ($\beta = -0.972$), followed by NDVI ($\beta = -0.808$), while NDBIz showed a moderate positive coefficient ($\beta = 0.470$). However, NDVI and NDWI also exhibited strong covariance within the study area, indicating substantial overlap in the vegetation and moisture-related spatial characteristics represented by the two indices. Consequently, standardised coefficient magnitudes should not be interpreted as independent measures of ecological importance.

Temporal coefficients further indicated substantial interannual variability in thermal conditions relative to the reference year (2000). Positive coefficients for 2005, 2010, 2015, and 2020 indicate comparatively stronger thermal conditions during these years, with 2020 exhibiting the strongest positive temporal effect ($\beta = 0.491$). In contrast, 2025 exhibited a weak negative temporal coefficient ($\beta = -0.115$) relative to 2000.

Overall, the regression results indicate that Ahmedabad's urban thermal variability was associated with vegetation cover, built-up intensity, temporal variability, and broader environmental heterogeneity across the study period.

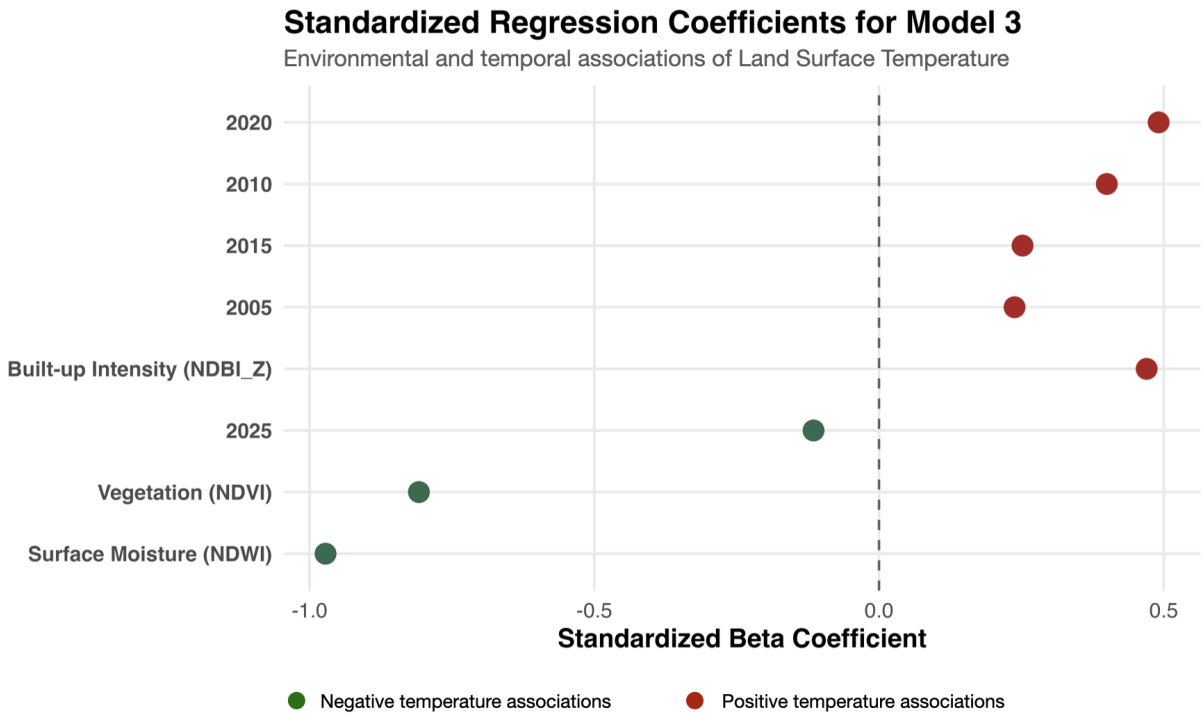

Figure 6. Standardised regression coefficients for Model 3 showing the direction and relative magnitude of modeled associations between vegetation cover (NDVI), surface moisture conditions (NDWI), standardised built-up intensity (NDBIz), and temporal year effects on land surface temperature (LST) across Ahmedabad between 2000 and 2025. Negative coefficients indicate inverse relationships with land surface temperature, whereas positive coefficients indicate positive temperature associations relative to the reference year (2000).

4.5 Relationship Between Vegetation and Built-up Intensity

The relationship between vegetation cover (NDVI), built-up intensity (NDBIz), and land surface temperature was further examined to evaluate how thermal conditions varied across differing levels of urbanization (Figure 7).

Across all levels of built-up intensity, increasing NDVI values were associated with lower predicted land surface temperatures. Areas characterised by higher NDBIz values consistently exhibited higher predicted temperatures relative to areas with lower built-up intensity across comparable NDVI ranges. The observed relationship pattern indicates that vegetation cover and built-up intensity showed concurrent relationships with urban thermal conditions throughout the study area.

Relationship between Vegetation Cover and Built-up intensity and LST

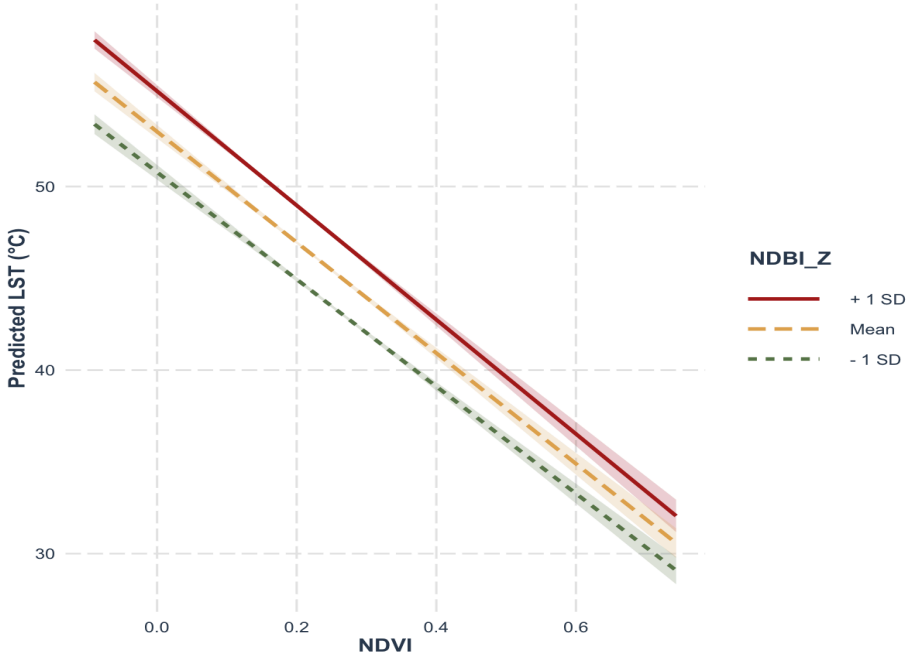

Figure 7. Relationship between vegetation cover (NDVI), standardised built-up intensity (NDBIz), and land surface temperature (LST) across Ahmedabad between 2000 and 2025. The figure illustrates conditional variation in NDVI–LST relationships across differing levels of built-up intensity within the study area.

Although NDVI maintained a negative relationship with land surface temperature across all built-up conditions, highly urbanised sectors generally retained elevated thermal conditions relative to less built-up environments.

Overall, the relationship pattern analysis indicates that both vegetation cover and built-up intensity contributed to spatial variation in land surface temperature across Ahmedabad between 2000 and 2025.

5. Discussion

5.1 Urban Expansion and Thermal Intensification

Foundational urban climate research has long established that replacement of natural land surfaces with impervious urban materials alters surface energy balance, reduces evapotranspiration, and increases heat storage within metropolitan environments (Oke, 1982; Voogt and Oke, 2003). From an ecological perspective, urban expansion also restructures the spatial continuity and functional capacity of vegetated surfaces that regulate localised thermal conditions through shading, evapotranspiration, and moisture retention (Weng et al., 2004; Yuan and Bauer, 2007). The Ahmedabad results strongly suggest that metropolitan growth between 2000 and 2025 was associated with substantial changes in the city's spatial thermal reorganisation through sustained impervious expansion and reduction of natural surface continuity.

Spatial and statistical analyses consistently indicated that increasing built-up intensity was associated with stronger thermal amplification across the metropolitan region. Elevated land surface temperatures remained concentrated within densely urbanised eastern and central sectors, while regression analyses indicated increasingly strong positive relationships between built-up intensity and LST through time (Figures 2, 3, and 6). Areas retaining greater vegetation continuity, particularly peri-river and peripheral zones, consistently exhibited comparatively moderated thermal conditions (Figure 2). Similar relationships between impervious expansion, ecological restructuring, and urban thermal intensification have been reported in recent studies examining landscape heterogeneity and metropolitan heat dynamics within rapidly urbanising regions (Chen et al., 2022; Gao et al., 2025; Ramachandra et al., 2025; Wu et al., 2026)

The temporal evolution of land surface temperature further suggests that Ahmedabad underwent successive phases of thermal transformation during the study period. Mean LST increased substantially between 2000 and 2020 before declining in 2025 (Table 1). However, the spatial distribution of thermal hotspots indicates that elevated thermal conditions remained widespread across major urban sectors despite localised increases in vegetation cover during later years (Figures 2 and 3). This persistence suggests that long-term impervious consolidation may produce enduring thermal structures that are not easily moderated through localised increases in vegetation alone.

The pronounced thermal continuity and elevated surface temperatures observed during 2010 may also have been partially amplified by the severe Ahmedabad heatwave event of May 2010, during which prolonged extreme temperature conditions approaching 47°C were recorded across Gujarat (Azhar et al., 2014) Because the present study utilised pre-monsoon summer Landsat imagery, regional heatwave conditions likely intensified thermal signatures captured across densely built-up sectors. The extensive elevated thermal concentration visible in the 2010 LST maps (Figure 2) further suggests that extreme climatic events may interact with impervious urban structure to intensify thermal stress within semi-arid metropolitan environments.

Recent assessments of urban heat island dynamics in India similarly indicate that rapidly expanding metropolitan regions are increasingly characterised by intensified thermal exposure associated with impervious expansion, ecological disturbance, and uneven land-cover transformation (Islam et al., 2024; Mandal and Chanda, 2025; Manna et al., 2026). The Ahmedabad results align closely with these broader national patterns while also highlighting how semi-arid climatic conditions may amplify sensitivity to ecological transformation under continued urban growth.

Overall, the findings indicate that Ahmedabad's urbanization process progressively was associated with increasing spatial thermal heterogeneity and persistent urban thermal concentration.

5.2 Temporal Variation in Vegetation - Temperature Relationships

Urban vegetation is widely recognised as one of the primary ecological mechanisms regulating urban thermal conditions through evapotranspiration, shading, and modification of localised surface energy balance (Weng et al., 2004; Yuan and Bauer, 2007). Recent urban ecological research further emphasizes that the cooling effectiveness of vegetation depends not only on vegetation quantity, but also on ecological connectivity, spatial configuration, and surrounding urban morphology (Chen et al., 2014; Gholamian Moghaddam et al., 2025; Yuan and Bauer, 2007). The Ahmedabad results indicate that the relationship between vegetation presence and thermal mitigation became increasingly complex under continued urban expansion. Although NDVI values exhibited localised increases after 2010 and reached their highest levels by 2025 (Figure 3; Table 1), the negative relationship between vegetatedl surfaces and land surface temperature became progressively more heterogeneous across the metropolitan region.

This divergence between vegetation abundance and thermal response suggests that persistence of vegetation cover alone was insufficient to maintain equivalent levels of vegetation-associated temperature moderation within the evolving urban landscape. Earlier phases of urban development exhibited comparatively clearer thermal separation between vegetated and highly built-up surfaces,

producing stronger and more coherent NDVI–LST relationships across Ahmedabad (Figure 5). In later years, however, similar NDVI ranges exhibited substantially broader thermal variability, particularly within dense urban sectors. The density distributions shown in Figure 5 therefore suggest increasing decoupling between vegetation presence and predictable thermal buffering under intensified urbanization.

Importantly, the relationship analyses did not indicate complete loss of vegetation-related cooling effects. Across all levels of built-up intensity, increasing NDVI remained associated with lower predicted land surface temperatures (Figure 7). However, highly urbanised sectors consistently retained comparatively elevated thermal conditions across comparable NDVI ranges. This pattern suggests that vegetation-associated thermal relationships increasingly occurred within thermally altered urban context shaped by impervious surface concentration and fragmented ecological structure.

The Ahmedabad findings further indicate that continued impervious expansion progressively constrained the spatial effectiveness of ecological thermal buffering across the metropolitan region. egetated surfaces located within lower-density and peri-urban environments maintained comparatively clearer vegetation–temperature relationships, whereas densely urbanised sectors exhibited greater thermal dispersion and more variable thermal responses. (Figures 2 and 5). Similar patterns have been documented in recent studies showing that fragmented vegetation structure and increasing landscape heterogeneity reduce the consistency of ecosystem-mediated thermal regulation within rapidly urbanising cities (Jha et al., 2026; Ramachandra et al., 2025; Wu et al., 2026).

Recent landscape ecology and urban morphology research likewise emphasizes that thermal regulation within metropolitan environments emerges through interactions between ecological surfaces and built-up spatial structure rather than through isolated land-cover effects alone (Chen et al., 2022; Ramsay et al., 2023; Zhang et al., 2026). The Ahmedabad results align closely with this perspective. Spatial analyses revealed that areas characterised by fragmented vegetation continuity and elevated built-up intensity exhibited increasingly heterogeneous thermal conditions despite localised increases in NDVI during later years of the study period (Figures 2 and 3). The standardised regression results further indicated persistent negative associations between NDVI, NDWI, and land surface temperature (Figure 6), although strong covariance between NDVI and NDWI limits interpretation of their independent ecological contributions.

The increase in vegetation cover observed after 2015 therefore should not necessarily be interpreted as direct ecological recovery in thermal terms. While western Ahmedabad and peri-urban sectors retained or expanded vegetated surfaces, continued urban densification and impervious consolidation likely reduced the broader landscape-scale expression of vegetation-associated temperature moderation across the

metropolitan region. Similar trends have been observed in rapidly expanding semi-arid cities where vegetation persistence alone was insufficient to offset increasing anthropogenic thermal influence under continued urban growth (Gholamian Moghaddam et al., 2025; Wang et al., 2018).

Overall, the findings suggest that Ahmedabad experienced increasingly heterogeneous urban thermal relationships under continued urbanization. Vegetation-associated thermal relationships remained evident throughout the study period, but their spatial expression became progressively more uneven and dependent on surrounding urban landscape conditions.

5.3 Spatial Heterogeneity in Urban Thermal Patterns

Recent urban climate and landscape ecology research increasingly emphasizes that urban heat island dynamics emerge through spatially differentiated and morphology-dependent processes rather than through uniform metropolitan warming. Variations in landscape configuration, development density, ecological connectivity, and surface composition can produce highly localised thermal responses within rapidly urbanising cities (Cao et al., 2026; Chen et al., 2022; Hernández-Herráez et al., 2025; Wan et al., 2026) The Ahmedabad results strongly reflect this pattern of spatial thermal heterogeneity.

Spatial analyses revealed pronounced contrasts between eastern industrialised sectors, western urban development corridors, peri-urban transitional landscapes, and river-associated ecological zones (Figure 2). Eastern and southeastern portions of the metropolitan region consistently exhibited stronger thermal concentration and higher built-up intensity, whereas parts of western Ahmedabad retained comparatively moderated thermal conditions despite continued urban expansion. These spatial differences suggest that localised urban form and ecological surface organization played a substantial role in shaping thermal behavior across the city.

Foundational urban climate research has long demonstrated that variations in urban structure and surface composition directly influence localised energy balance processes and heat exchange within cities (Voogt and Oke, 2003). More recent studies further indicate that urban geometry, ecological fragmentation, and spatial configuration may exert stronger influence on intra-urban thermal variability than urban expansion intensity alone, particularly within morphologically heterogeneous metropolitan regions (Wan et al., 2026; Wu et al., 2026). The Ahmedabad findings align closely with this interpretation, especially in relation to the contrasting thermal trajectories observed between compact eastern sectors and comparatively greener western development corridors (Figure 2).

The peri-urban environments identified in the spatial analyses further highlight the transitional ecological character of Ahmedabad's thermal evolution. These landscapes frequently exhibited mixed thermal signatures characterised by coexistence of residual vegetation cover, expanding impervious surfaces, and

moderate thermal intensification (Figures 2 and 5). Similar morphology-driven transitional thermal structures have been identified in recent studies emphasising the role of fragmented land-cover organization and ecological patch dynamics in shaping localised heat accumulation patterns within rapidly urbanising environments (De-La-Cruz et al., 2025; Ramachandra et al., 2025).

The increasing thermal variability observed across Ahmedabad also suggests that future urban heat exposure may become progressively more uneven across the metropolitan region. The widening thermal dispersion observed within comparable NDVI ranges (Figure 5) indicates that localised urban conditions increasingly modified the thermal response of ecological surfaces through time. Recent work examining highly heterogeneous interactions between urban structure and localised warming similarly demonstrates that thermal amplification can vary substantially across different urban forms, ecological configurations, and climatic subregions within the same metropolitan area (Kong et al., 2024; Ramsay et al., 2023).

Importantly, the Ahmedabad results suggest that ecological continuity remained a critical moderating factor on localised thermal conditions even under continued urban growth. River-associated landscapes, peri-urban vegetated zones, and lower-density ecological surfaces consistently exhibited comparatively moderated thermal signatures relative to densely compacted urban sectors (Figure 2). These findings reinforce the argument that ecological persistence within rapidly urbanising metropolitan regions continues to play an important role in regulating localised thermal stress despite increasing impervious expansion.

Overall, the findings indicate that Ahmedabad evolved into a spatially differentiated ecological thermal landscape characterised by increasingly heterogeneous urban heat patterns shaped by varying development trajectories, land-cover configurations, ecological fragmentation, and localised urban morphology across the metropolitan region.

5.4 Implications for Climate-Sensitive Urban Planning

The findings of the present study suggest that mitigation of urban thermal stress within rapidly expanding semi-arid cities requires approaches that extend beyond simple increases in vegetation quantity alone. Although vegetation consistently maintained a negative relationship with land surface temperature across Ahmedabad (Figures 4 and 5), the spatial analyses indicated that thermal relationships varied substantially according to surrounding urban conditions, built-up intensity, and ecological landscape structure (Figures 2 and 7). This indicates that the thermal performance of urban ecological systems depends not only on the presence of green surfaces, but also on their spatial integration within the broader metropolitan environment.

Recent research on urban green infrastructure similarly emphasizes that fragmented or spatially isolated vegetation

may provide limited landscape-scale thermal regulation under highly urbanised conditions (Chen et al., 2014; Jha et al., 2026; Zhang et al., 2026). Studies examining ecological cooling performance increasingly argue that vegetation connectivity, patch configuration, and integration with surrounding urban morphology are critical determinants of effective urban heat mitigation (Hernández-Herráez et al., 2025; Zhang et al., 2026). The Ahmedabad results align closely with this perspective, particularly in relation to the weaker and more spatially variable vegetation–temperature relationships observed within densely urbanised sectors despite localised increases in NDVI during later years of the study period (Figures 3 and 5).

The results further suggest that future urban planning strategies within Ahmedabad must treat thermal regulation as a spatial ecological challenge rather than solely as a land-cover management issue. Areas characterised by dense impervious development and fragmented ecological continuity consistently exhibited stronger thermal amplification throughout the study period, whereas comparatively moderated thermal conditions were retained within sectors containing greater vegetation integration and lower built-up concentration (Figure 2). These patterns indicate that urban morphology and ecological configuration are associated with the spatial distribution of thermal stress across the metropolitan landscape.

Recent sustainability-focused urban climate studies similarly emphasize that climate-sensitive planning requires coordinated integration of ecological infrastructure, urban morphology, and land-use planning in order to improve long-term thermal resilience within rapidly urbanising cities (Gao et al., 2025; Jha et al., 2026; Ramsay et al., 2023). Within highly compact urban environments, isolated greening interventions may therefore provide limited thermal benefit if continued impervious consolidation and ecological fragmentation simultaneously intensify anthropogenic heat accumulation.

The semi-arid climatic setting of Ahmedabad further increases the importance of preserving ecologically functional vegetated surfaces under future urban expansion. The strong negative associations observed for both NDVI and NDWI in the standardised regression analysis (Figure 6) further suggest that moisture-retaining ecological surfaces may play an important role in moderating thermal conditions within semi-arid urban environments. Recent assessments of urban heat island dynamics in India indicate that rapidly growing metropolitan regions are becoming increasingly vulnerable to persistent thermal stress due to combined pressures of climatic warming, impervious expansion, and ecological degradation (Gholamian Moghaddam et al., 2025; Islam et al., 2024; Mandal and Chanda, 2025). In this context, preservation of ecological continuity, peri-urban vegetation structure, and river-associated green corridors may become increasingly important for maintaining long-term urban thermal resilience.

Overall, the findings indicate that climate-sensitive urban planning in

Ahmedabad should prioritize not only preservation of vegetation quantity, but also the spatial connectivity, ecological functionality, and landscape-scale integration of cooling surfaces within the metropolitan environment.

5.5 Limitations and Future Research

Several limitations should be considered when interpreting the findings of the present study. First, the analysis was based on multi-temporal Landsat imagery acquired during pre-monsoon summer conditions. Although this enabled relatively consistent comparison of peak seasonal thermal conditions, land surface temperature may vary substantially due to climatic variability, atmospheric conditions, antecedent moisture, acquisition-date differences, and short-term extreme weather events. The elevated thermal conditions observed during 2010, for example, were likely influenced not only by urban expansion but also by the severe Ahmedabad heatwave occurring near the image acquisition period.

Second, the study evaluated land surface temperature (LST) rather than near-surface air temperature. While satellite-derived LST provides valuable insight into spatial thermal variability and surface energy dynamics, it does not directly represent pedestrian-level thermal exposure or physiological heat stress. Consequently, the findings primarily reflect landscape-scale thermal behavior associated with land-cover transformation and urban morphology rather than direct human thermal conditions.

The analysis was additionally constrained by the spatial and temporal resolution of Landsat imagery. Although Landsat provides one of the most effective long-term archives for multi-decadal urban environmental analysis, finer-scale thermal variability associated with street canyons, localised vegetation patches, and microclimatic processes may not be fully captured at 30 m resolution. Similarly, the use of five-year intervals limits evaluation of shorter-term climatic fluctuations and nonlinear phases of urban expansion. In addition, the 2005 analysis utilised Landsat 7 ETM+ imagery acquired after the Scan Line Corrector (SLC) failure, which may have introduced residual spatial inconsistencies despite preprocessing and compositing procedures.

Several methodological limitations should also be acknowledged. The study relied on NDVI, NDWI, and NDBI-derived spectral indices as generalised proxies for vegetation cover, surface moisture, and built-up intensity. While widely used in urban thermal studies, these indices cannot fully capture ecological quality, vertical urban form, surface material properties, or anthropogenic heat emissions. Furthermore, the use of standardised NDBIz values improved inter-sensor comparability across Landsat generations but limited direct interpretation of absolute temporal changes in built-up magnitude.

The regression analyses also did not explicitly account for spatial autocorrelation among sampled pixels. Because neighboring urban surfaces often exhibit similar thermal and ecological characteristics, statistical

independence assumptions may have been partially violated, potentially inflating significance estimates. Consequently, the reported relationships should be interpreted primarily as spatially descriptive associations rather than strictly causal relationships. Strong covariance between NDVI and NDWI ($r = -0.96$) additionally introduced elevated multicollinearity, limiting fully independent interpretation of coefficient magnitude and relative predictor importance.

Finally, the study focused primarily on horizontal land-cover structure and did not incorporate three-dimensional urban morphology variables such as building height, sky-view factor, or urban canyon geometry, which also influence urban thermal behavior. Future research could therefore benefit from integration of higher-resolution thermal datasets, Local Climate Zone (LCZ) frameworks, spatial regression approaches, urban canopy modeling, ecological landscape metrics, and socio-economic variables to improve understanding of thermal variability and heat exposure within rapidly urbanising semi-arid cities.

6. Conclusion

Using the Google Earth Engine (GEE) cloud platform and multi-temporal Landsat imagery, this study examined long-term variation in land surface temperature (LST), vegetation cover, and built-up expansion across Ahmedabad between 2000 and 2025. Spatial analysis revealed progressive expansion of high-temperature urban zones alongside increasing spatial heterogeneity in thermal conditions across the metropolitan region. Elevated thermal conditions remained concentrated primarily within densely urbanised eastern and central sectors, whereas comparatively moderated thermal patterns were more consistently observed within peri-urban landscapes, river-associated environments, and parts of western Ahmedabad containing greater vegetation continuity.

The analyses further indicated persistent negative relationships between vegetation cover and land surface temperature, while built-up intensity remained positively associated with elevated thermal conditions across Ahmedabad. However, vegetation–temperature relationships became increasingly heterogeneous through time, with later years exhibiting broader thermal variability across comparable NDVI ranges despite localised increases in vegetation cover. These findings suggest that vegetation persistence alone may be insufficient to maintain consistent temperature moderation under continued urban densification and fragmented ecological structure.

The study additionally demonstrated that Ahmedabad's urban thermal environment evolved through increasingly differentiated spatial patterns shaped by variation in built-up intensity, vegetation distribution, peri-urban transition, and urban landscape configuration. The observed widening of thermal variability across the metropolitan region highlights the importance of considering spatial ecological structure and urban morphology alongside land-cover quantity in understanding long-term urban

thermal conditions within rapidly expanding semi-arid cities.

Overall, this study contributes a multi-decadal assessment of urban thermal variation in Ahmedabad and highlights the value of integrating long-term remote sensing analysis with spatial ecological interpretation in urban climate research. The findings further suggest that climate-sensitive urban planning strategies in rapidly urbanising semi-arid environments should prioritize not only preservation and expansion of urban vegetation, but also improvement of ecological continuity, spatial connectivity, and integration of vegetated surfaces within the broader metropolitan landscape.

7. References

Alcoforado, M.J., Andrade, H., 2008. Global Warming and the Urban Heat Island, in: Marzluff, J.M., Shulenberger, E., Endlicher, W., Alberti, M., Bradley, G., Ryan, C., Simon, U., ZumBrunnen, C. (Eds.), Urban Ecology: An International Perspective on the Interaction Between Humans and Nature. Springer US, Boston, MA, pp. 249–262. https://doi.org/10.1007/978-0-387-73412-5_14

Azhar, G.S., Mavalankar, D., Nori-Sarma, A., Rajiva, A., Dutta, P., Jaiswal, A., Sheffield, P., Knowlton, K., Hess, J.J., on behalf of the Ahmedabad HeatClimate Study Group, 2014. Heat-Related Mortality in India: Excess All-Cause Mortality Associated with the 2010 Ahmedabad Heat Wave. PLoS ONE 9, e91831. https://doi.org/10.1371/journal.pone.0091831

Cao, S., Wu, Z., Yu, Z., Ouyang, W., Tong, Z., 2026. Integrating urban morphology and thermal environment characteristics for urban form classification: A case study of Nanjing, China. Energy Build. 117585. https://doi.org/10.1016/j.enbuild.2026.117585

Chen, A., Yao, X.A., Sun, R., Chen, L., 2014. Effect of urban green patterns on surface urban cool islands and its seasonal variations. Urban For. Urban Green. 13, 646–654. https://doi.org/10.1016/j.ufug.2014.07.006

Chen, Y., Shan, B., Yu, X., 2022. Study on the spatial heterogeneity of urban heat islands and influencing factors. Build. Environ. 208, 108604. https://doi.org/10.1016/j.buildenv.2021.108604

De-La-Cruz, J., Solano-Reynoso, W., Moncada, W., Soca-Flores, R., Carrasco-Badajoz, C., Rayme-Chalco, C., Lizarbe-Alarcón, H., León-Palacios, E., Tenorio-Huarancca, D., Lozano, J., 2025. Surface Heat Island and Its Link to Urban Morphology: Multitemporal Analysis with Landsat Images in an Andean City in Peru. Urban Sci. 9, 507. https://doi.org/10.3390/urbansci9120507

Gao, W., Liu, J., Li, S., Xu, K., Wang, M., Xia, Z., 2025. Effect of urban morphology on local-scale urban heat island intensity under varying urbanisation: A case study of Wuhan. Sustain. Cities Soc. 125, 106328. https://doi.org/10.1016/j.scs.2025.106328

Gholamian Moghaddam, I., Sarvari, H., Saeidi Mofrad, S., Ghanbarzade Darban, H., 2025. Green infrastructure’s impact on thermal condition in arid & semi-arid cities: a systematic review. Creat. City Des. 8. https://doi.org/10.57647/J.CCD.2025.0801.01

Gorelick, N., Hancher, M., Dixon, M., Ilyushchenko, S., Thau, D., Moore, R., 2017. Google Earth Engine: Planetary-scale geospatial analysis for everyone. Big Remote. Sensed Data Tools Appl. Exp. 202, 18–27. https://doi.org/10.1016/j.rse.2017.06.031

Gupta, A., Sadab, A., De, B., 2024. Assessment of critical thermal characteristics and land surface dynamics of an Indian metropolitan city. J. Water Clim. Change 15, 3409–3430. https://doi.org/10.2166/wcc.2024.370

Gupta, R.K., 2025. Spatial dynamics of micro-urban heat islands and satellite-derived indices of Ahmedabad City, India. J. Earth Syst. Sci. 134, 23. https://doi.org/10.1007/s12040-024-02493-y

Hernández-Herráez, G., Martínez-Lastras, S., Lagüela, S., Martín-Jiménez, J.A., Del Pozo, S., 2025. Morphological and Environmental Drivers of Urban Heat Islands: A Geospatial Model of Nighttime Land Surface Temperature in Iberian Cities. Appl. Sci. 15, 6093. https://doi.org/10.3390/app15116093

Hurduc, A., Ermida, S.L., DaCamara, C.C., 2024. On the Suitability of Different Satellite Land Surface Temperature Products to Study Surface Urban Heat Islands. Remote Sens. 16, 3765. https://doi.org/10.3390/rs16203765

Islam, S., Karipot, A., Bhawar, R., Sinha, P., Kedia, S., Khare, M., 2024. Urban heat island effect in India: a review of current status, impact and mitigation strategies. Discov. Cities 1, 34. https://doi.org/10.1007/s44327-024-00033-3

Jha, P., Yadav, P.K., Joy, M.S., Jha, A.N., Bansal, T., Alkhuraiji, W.S., Zhran, M., 2026. Urban Cooling Under Extreme Heat: The Role of Blue-Green Spaces as Nature-Based Solutions in Delhi. Sustainability 18, 2378. https://doi.org/10.3390/su18052378

Joshi, R., Raval, H., Pathak, M., Prajapati, S., Patel, A., Singh, V., Kalubarme, M.H., 2015. Urban Heat Island Characterization and Isotherm Mapping Using Geo-Informatics Technology in Ahmedabad City, Gujarat State, India. Int. J. Geosci. 06, 274–285. https://doi.org/10.4236/ijg.2015.63021

Kayet, N., Pathak, K., Chakrabarty, A., Sahoo, S., 2016. Urban heat island explored by co-relationship between land surface temperature vs multiple vegetation indices. Spat. Inf. Res. 24, 515–529. https://doi.org/10.1007/s41324-016-0049-3

Kong, J., Zhao, Y., Gao, K., Strebel, D., Carmeliet, J., Lei, C., 2024. Highly inhomogeneous interactions between background climate and urban warming across typical local climate zones in heatwave and non-heatwave days. https://doi.org/10.48550/ARXIV.2405.17213

Mandal, N.S., Chanda, K., 2025. Investigation of Urban Heat Islands and modeling of Land Surface Temperature over selected Indian cities using MODIS products. Theor. Appl. Climatol. 156, 258. https://doi.org/10.1007/s00704-025-05480-5

Manna, H., Pramanik, M., Ahamed, R., Sarkar, S., 2026. Urban heat in Mumbai: From scenario analysis to the mitigation of nighttime thermal footprint. J. Urban Manag. S2226585626000415. https://doi.org/10.1016/j.jum.2026.02.008

Manorama Mohanty, Mrutyunjay Mohapatra, Vigin Lal F, Varun Gupta, Chanchal Devi, 2022. Climate of Ahmedabad. Indian Meteorological Department.

McFEETERS, S.K., 1996. The use of the Normalized Difference Water Index (NDWI) in the delineation of open water features. Int. J. Remote Sens. 17, 1425–1432. https://doi.org/10.1080/01431169608948714

Mohammad, P., Goswami, A., Bonafoni, S., 2019. The Impact of the Land Cover Dynamics on Surface Urban Heat Island Variations in Semi-Arid Cities: A Case Study in Ahmedabad City, India, Using Multi-Sensor/Source Data. Sensors 19. https://doi.org/10.3390/s19173701

Oke, T.R., 1982. The energetic basis of the urban heat island. Q. J. R. Meteorol. Soc. 108, 1–24. https://doi.org/https://doi.org/10.1002/qj.49710845502

Ramachandra, T.V., Rana, R.S., Vinay, S., Aithal, B.H., 2025. Urban heat island linkages with the landscape morphology. Sci. Rep. 15, 24485. https://doi.org/10.1038/s41598-025-09141-5

Ramsay, E.E., Duffy, G.A., Burge, K., Taruc, R.R., Fleming, G.M., Faber, P.A., Chown, S.L., 2023. Spatio-temporal development of the urban heat island in a socioeconomically diverse tropical city. Environ. Pollut. 316, 120443.

https://doi.org/https://doi.org/10.1016/j.envpol.2022.120443
Rouse, J.W., Jr., Haas, R.H., Schell, J.A., Deering, D.W., 1974. Monitoring Vegetation Systems in the Great Plains with Erts, in: NASA Special Publication. p. 309.
Roy, B., Bari, E., 2022. Examining the relationship between land surface temperature and landscape features using spectral indices with Google Earth Engine. Heliyon 8, e10668. https://doi.org/10.1016/j.heliyon.2022.e10668
Sharma, P., Yogeswaran, N., Singh, R., 2025. Longitudinal Study of Urban Heat Island Phenomena in Rapidly Developing Cities: The Case of Gurugram. Civ. Eng. Archit. 13, 2862–2875. https://doi.org/10.13189/cea.2025.130405
Singh, P., Verma, P., Chaudhuri, A.S., Singh, V.K., Rai, P.K., 2024. Evaluating the relationship between Urban Heat Island and temporal change in land use, NDVI and NDBI: a case study of Bhopal city, India. Int. J. Environ. Sci. Technol. 21, 3061–3072. https://doi.org/10.1007/s13762-023-05141-y
Stamou, A., Stylianidis, E., 2025. Urban Monitoring from the Cloud: A Review of Google Earth Engine (GEE)-Based Approaches for Assessing Urban Environmental Indices. Geographies 5, 68. https://doi.org/10.3390/geographies5040068
United States Geological Survey, 2020. Landsat Collection 2 Surface Temperature Product Guide. United States Geological Survey.
Voogt, J.A., Oke, T.R., 2003. Thermal remote sensing of urban climates. Remote Sens. Environ. 86, 370–384. https://doi.org/https://doi.org/10.1016/S0034-4257(03)00079-8
Wan, B., Shen, N., Zhang, H., Sheng, Q., 2026. Analyzing the impact of urban morphology on urban land surface temperature from the perspective of spatial configuration and explainable machine learning: A case study of seven cities. Sustain. Cities Soc. 138, 107165. https://doi.org/10.1016/j.scs.2026.107165
Wang, C., Middel, A., Myint, S.W., Kaplan, S., Brazel, A.J., Lukasczyk, J., 2018. Assessing local climate zones in arid cities: The case of Phoenix, Arizona and Las Vegas, Nevada. ISPRS J. Photogramm. Remote Sens. 141, 59–71. https://doi.org/10.1016/j.isprsjprs.2018.04.009
Weng, Q., Lu, D., Schubring, J., 2004. Estimation of land surface temperature–vegetation abundance relationship for urban heat island studies. Remote Sens. Environ. 89, 467–483. https://doi.org/10.1016/j.rse.2003.11.005
Wu, Y., Li, R., Hu, T., Wang, M., 2026. Exploring the effects of urban morphology and its spatial heterogeneity on LST: a quantitative analysis of seasonal and diurnal variations. J. Asian Archit. Build. Eng. 1–22. https://doi.org/10.1080/13467581.2026.2639787
Yuan, F., Bauer, M.E., 2007. Comparison of impervious surface area and normalized difference vegetation index as indicators of surface urban heat island effects in Landsat imagery. Remote Sens. Environ. 106, 375–386. https://doi.org/https://doi.org/10.1016/j.rse.2006.09.003
Zha, Y., Gao, J., Ni, S., 2003. Use of normalized difference built-up index in automatically mapping urban areas from TM imagery. Int. J. Remote Sens. 24, 583–594. https://doi.org/10.1080/01431160304987
Zhang, Y., Zhang, X., Yan, D., Wang, Y., Zhang, M., Li, Y., Wu, L., 2026. Quantifying the cooling effect of green spaces on urban heat island effect. Geomat. Nat. Hazards Risk 17, 2605714. https://doi.org/10.1080/19475705.2025.2605714

Supplementary Material

Spatiotemporal Evolution of Urban Thermal Conditions, Vegetation Dynamics, and Built-up Expansion in Ahmedabad, India (2000–2025) Using Multi-Temporal Landsat Analysis.

Contents

Supplementary Figures

Supplementary Tables

- Table S1. Pearson correlation matrix among environmental variables and land surface temperature (LST).
- Table S2. Year-wise Pearson correlation coefficients between environmental variables and land surface temperature (LST).
- Table S3. Variance inflation factor (VIF) statistics for environmental predictors.
- Table S4. Standardized regression coefficients for Model 3.
- Table S5. Year-wise regression model coefficients and adjusted R^2 values.

Supplementary Figures

Figure S1

Full temporal evolution of land surface temperature (LST) across Ahmedabad between 2000 and 2025.

This figure illustrates the spatial evolution of land surface temperature patterns across Ahmedabad using Landsat-derived thermal imagery for the years 2000, 2005, 2010, 2015, 2020, and 2025. The maps demonstrate progressive spatial restructuring of urban thermal conditions and expansion of high-temperature zones across densely urbanized sectors of the metropolitan region.

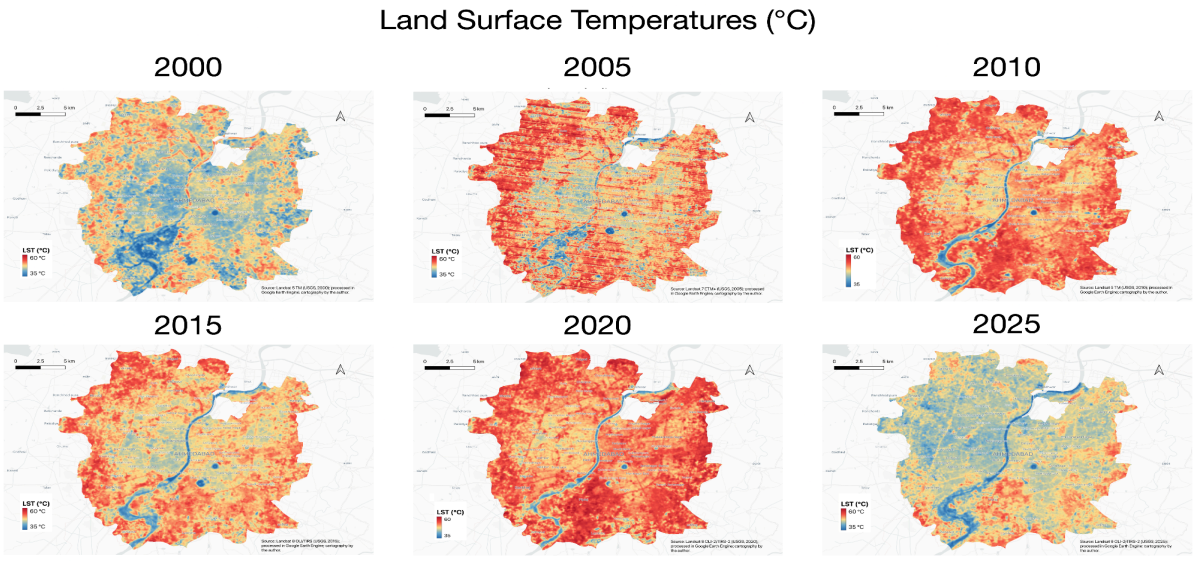

Figure S2

Full temporal evolution of vegetation cover (NDVI) across Ahmedabad between 2000 and 2025.

This figure illustrates the temporal evolution of vegetation greenness derived from the Normalized Difference Vegetation Index (NDVI). Spatial patterns demonstrate changing vegetation distribution across urban, peri-urban, and river-associated landscapes throughout the study period.

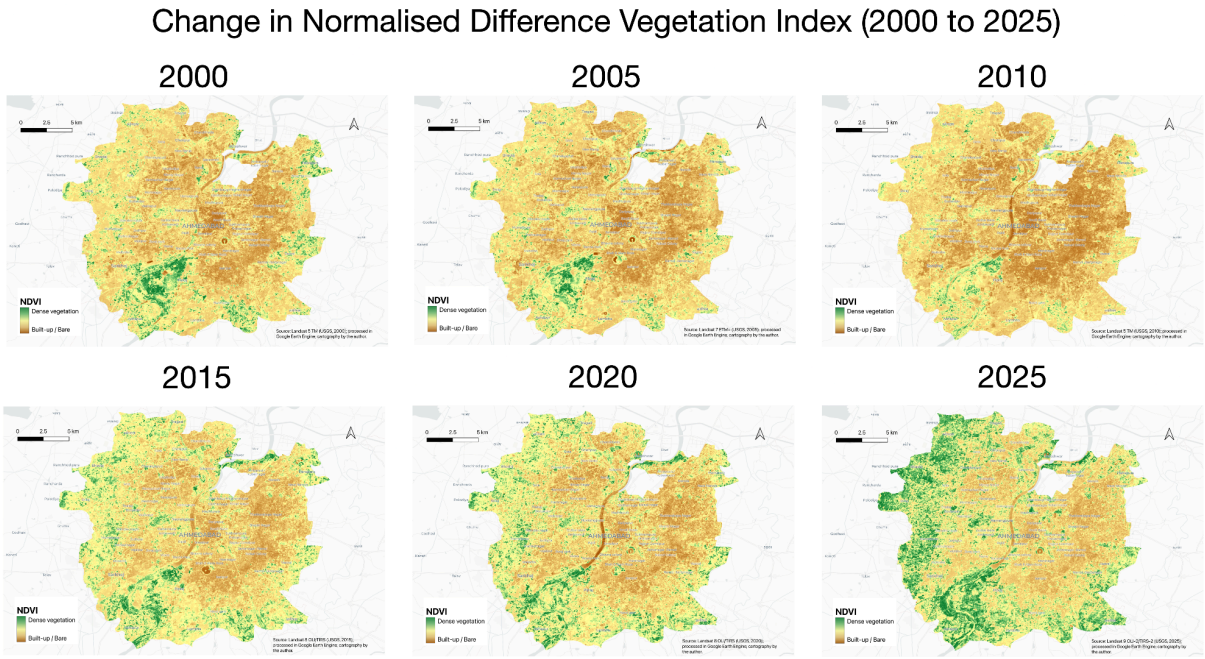

Figure S3

Full temporal evolution of standardized built-up intensity (NDBI_Z) across Ahmedabad between 2000 and 2025.

This figure illustrates the spatial evolution of relative built-up intensity across Ahmedabad using year-wise standardized NDBI (NDBI_Z) values. Positive values indicate areas with relatively higher built-up intensity within each year, whereas negative values indicate comparatively lower built-up intensity.

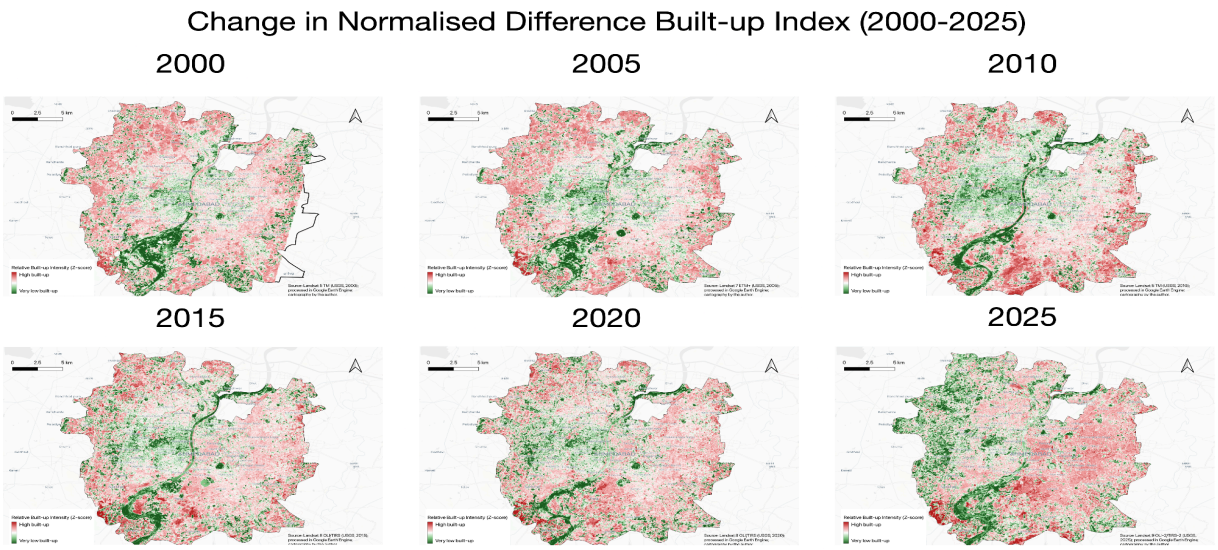

Figure S4

Temporal distribution of land surface temperature (LST) between 2000 and 2025.

Boxplots showing the temporal distribution and variability of land surface temperature across Ahmedabad for all study years.

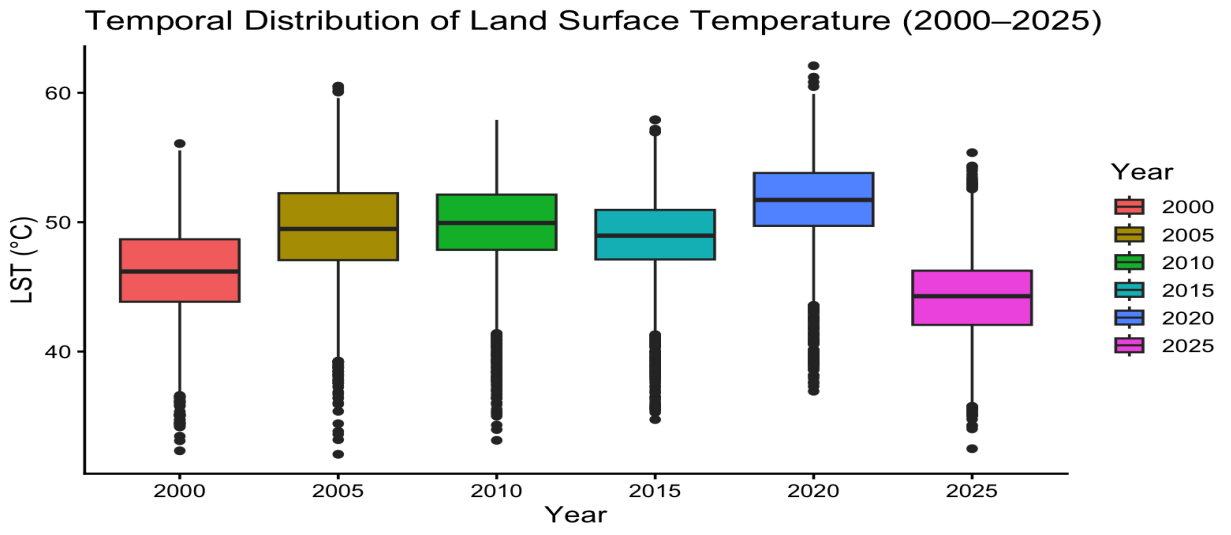

Figure S5

Temporal distribution of vegetation cover (NDVI) between 2000 and 2025.

Boxplots showing temporal variation in vegetation greenness across Ahmedabad throughout the study period.

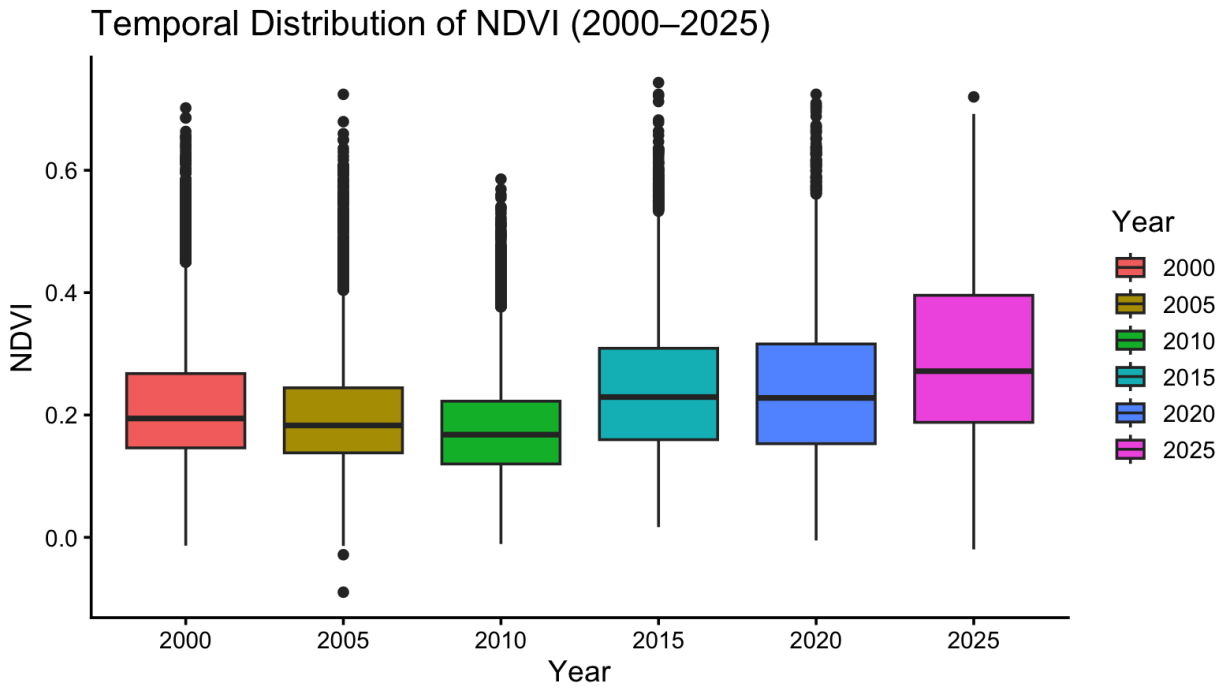

Figure S6

Temporal distribution of standardized built-up intensity (NDBI_Z) between 2000 and 2025.

Boxplots illustrating the temporal distribution of standardized built-up intensity across Ahmedabad.

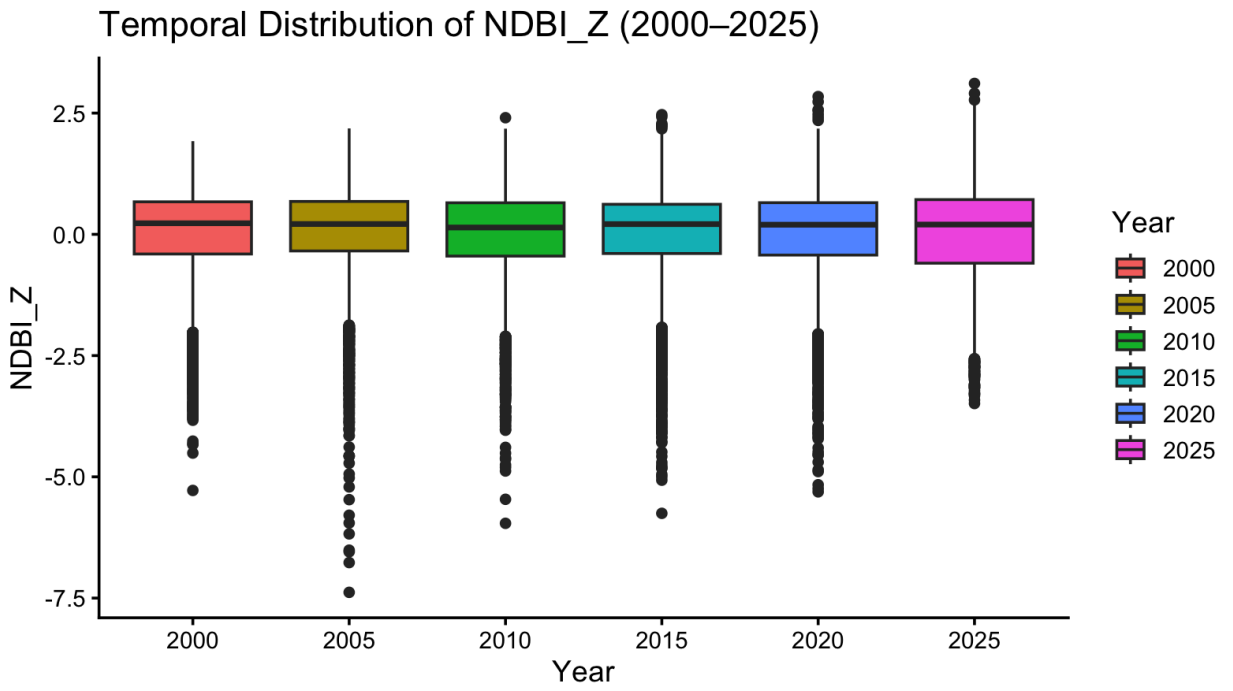

Figure S7

Temporal distribution of surface moisture conditions (NDWI) between 2000 and 2025.

Boxplots showing temporal variation in surface moisture conditions across Ahmedabad.

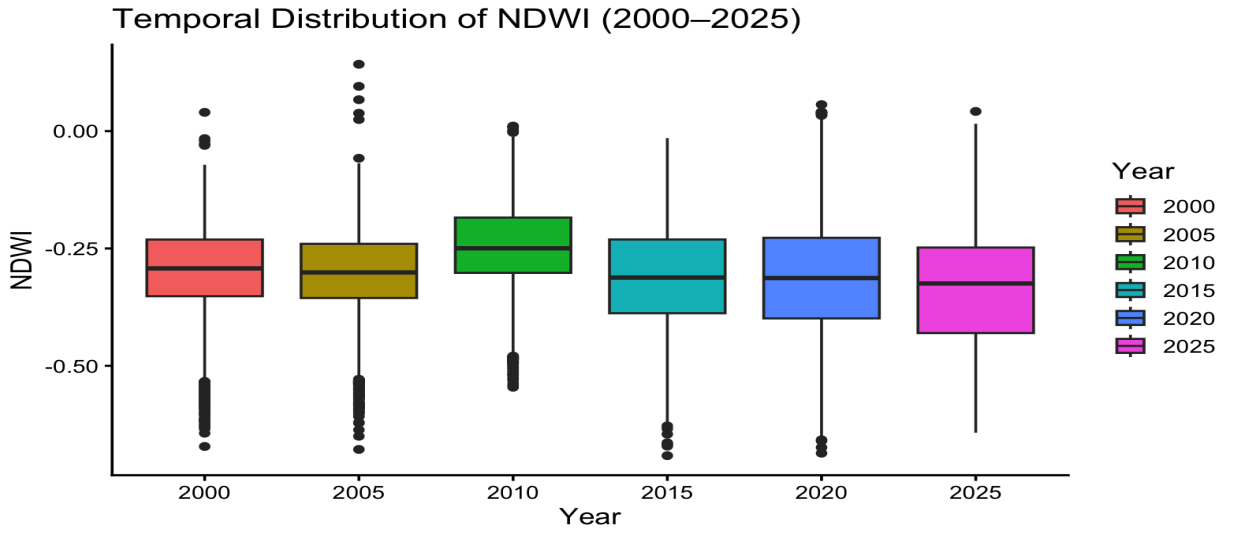

Figure S8

Relationship between NDVI and land surface temperature (LST) across Ahmedabad.

Scatterplot showing the relationship between vegetation greenness (NDVI) and land surface temperature across the study area.

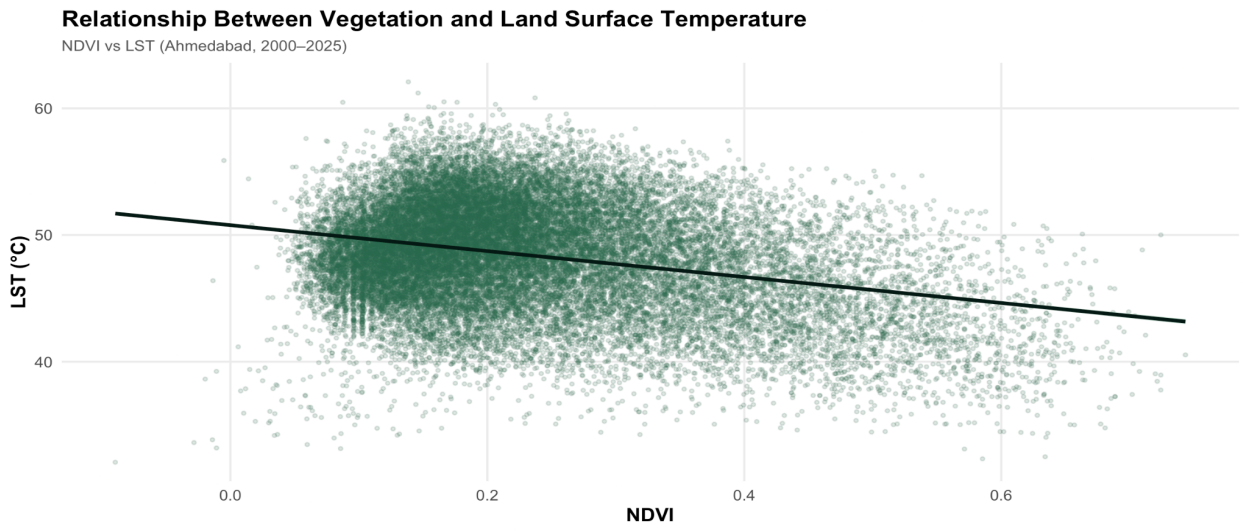

Figure S9

Relationship between NDBI_Z and land surface temperature (LST) across Ahmedabad.

Scatterplot showing the relationship between standardized built-up intensity (NDBI_Z) and land surface temperature.

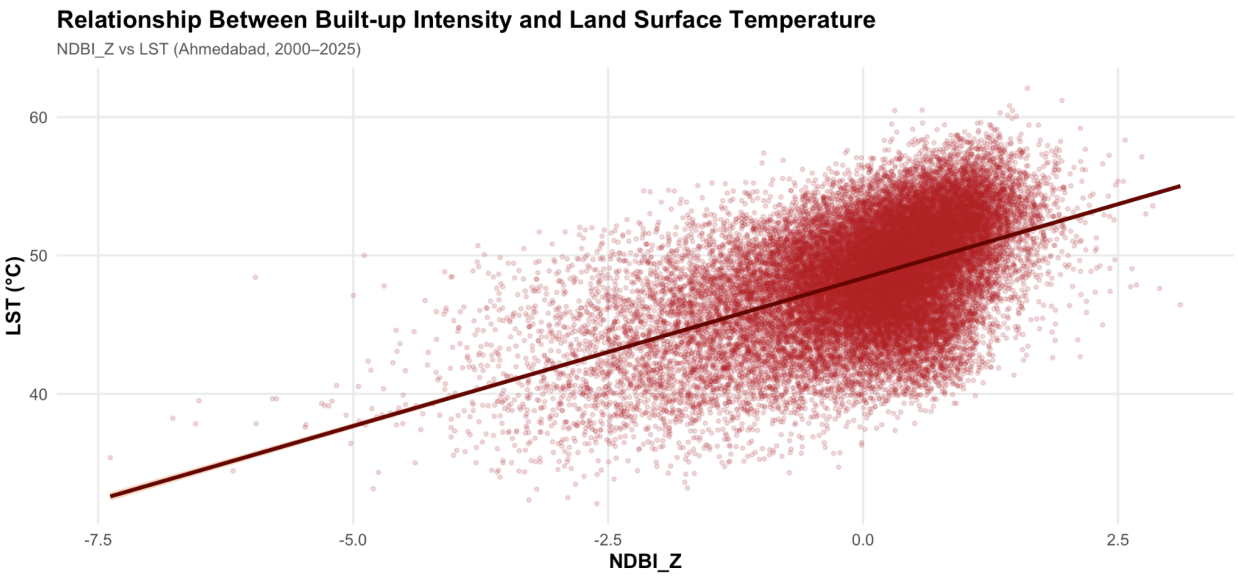

Figure S10

Relationship between NDWI and land surface temperature (LST) across Ahmedabad.

Scatterplot showing the relationship between surface moisture conditions (NDWI) and land surface temperature.

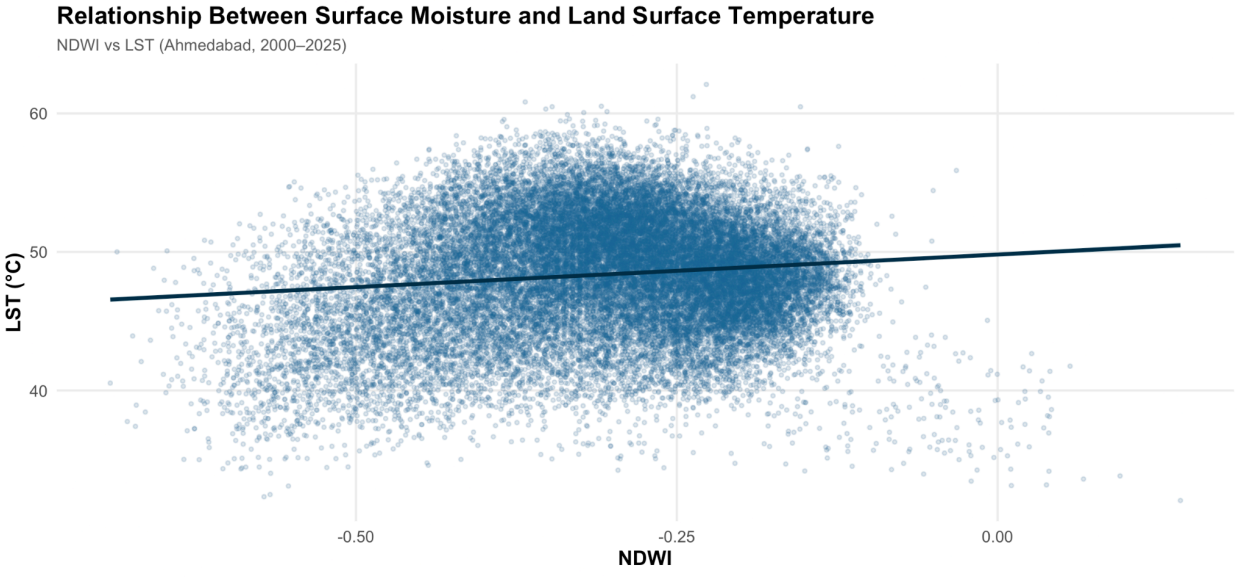

Figure S11

Regression diagnostic plots for Model 3.

Diagnostic plots used to evaluate regression assumptions for Model 3, including residual distribution, homoscedasticity, leverage, and model fit.

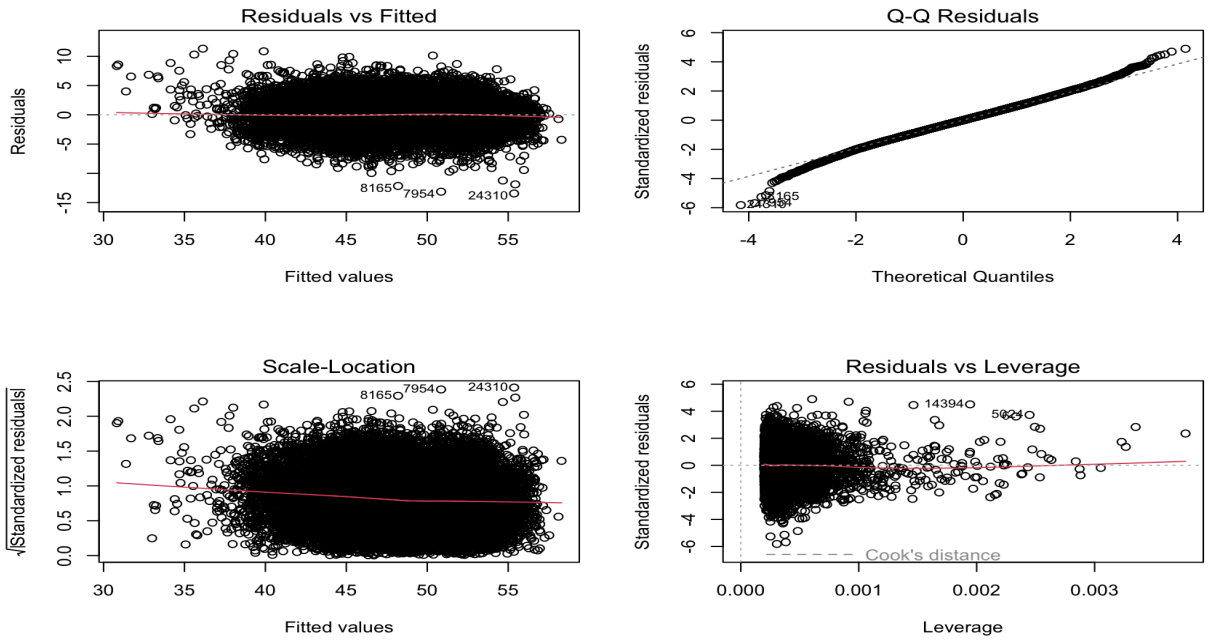

Figure S12

Temporal evolution of mean land surface temperature (LST) across Ahmedabad.

Temporal trend in mean land surface temperature between 2000 and 2025.

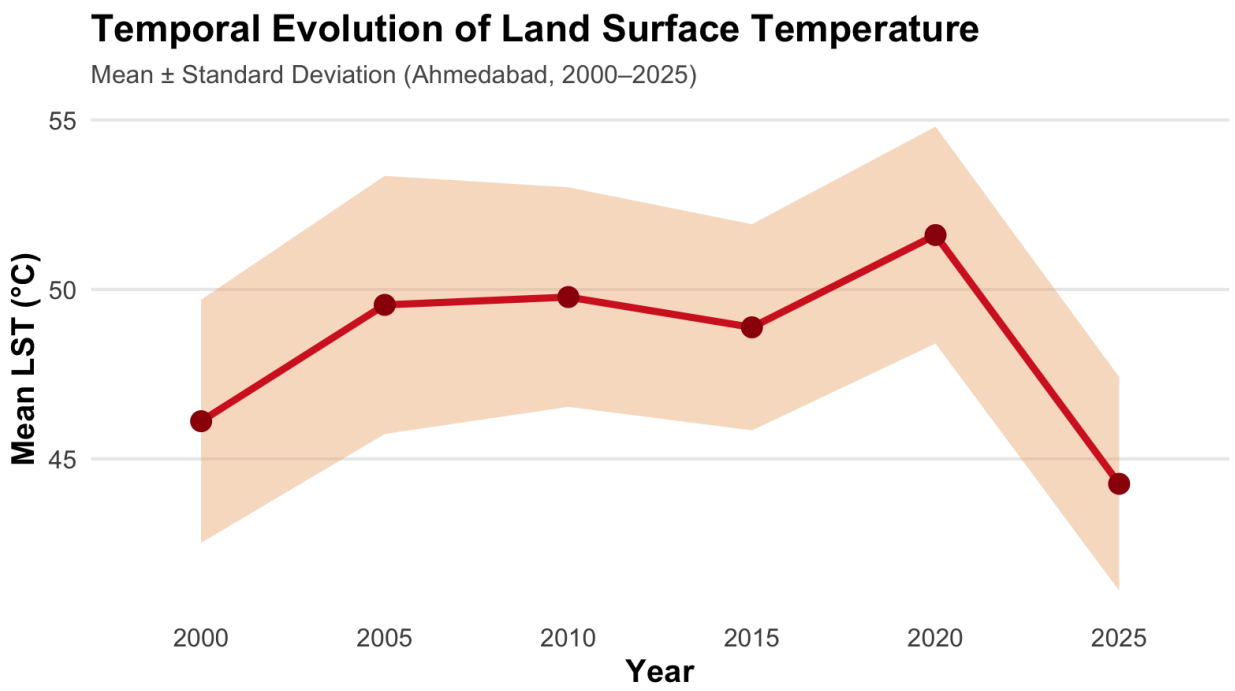

Figure S13

Temporal evolution of mean NDVI across Ahmedabad.

Temporal trend in average vegetation greenness across Ahmedabad between 2000 and 2025.

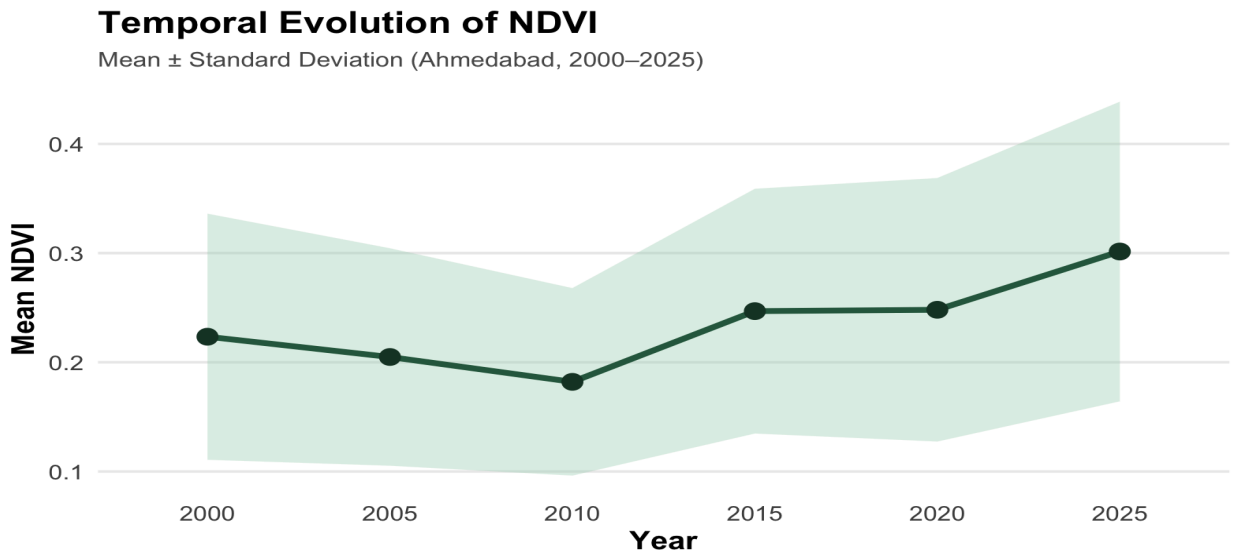

Figure S14

Temporal thermal effects relative to the baseline year (2000).

Regression-derived temporal coefficients showing relative thermal differences between each study year and the baseline year (2000).

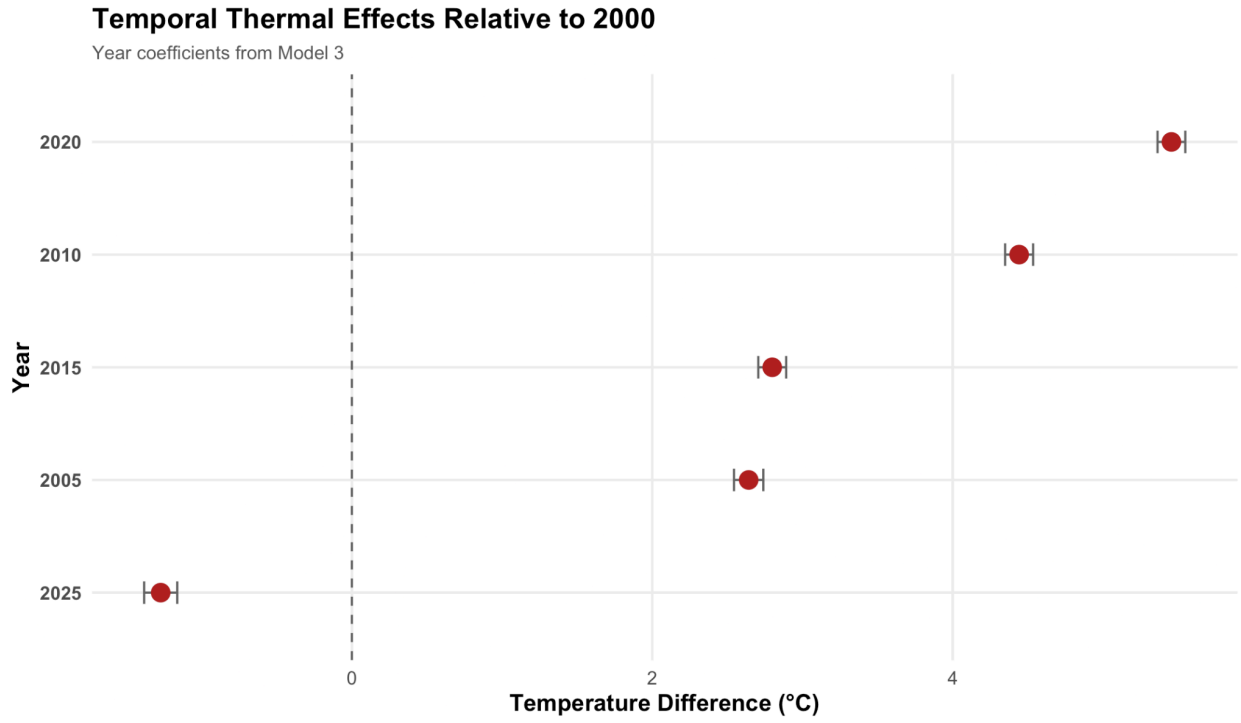

Supplementary Tables

Table S1

Pearson correlation matrix among environmental variables and land surface temperature (LST).

Variable	Correlation	CI Lower	CI Upper	P Value
NDVI vs LST	-0.293	-0.303	-0.282	0.00E+00
NDBI_Z vs LST	0.513	0.504	0.521	0.00E+00
NDWI vs LST	0.118	0.107	0.13	1.74E-93

Table S2

Year-wise Pearson correlation coefficients between environmental variables and land surface temperature (LST).

Year	NDVI_LST	NDBI_LST	NDWI_LST
2000	-0.432	0.677	0.259
2005	-0.337	0.694	0.094
2010	-0.15	0.679	-0.058
2015	-0.103	0.59	-0.081
2020	-0.185	0.626	0.005
2025	-0.246	0.51	0.153

Table S3

Variance inflation factor (VIF) statistics for environmental predictors.

This table presents multicollinearity diagnostics for environmental predictors included in the regression models.

Variable	VIF	Interpretation
NDVI	22.545	Severe
NDBI_Z	2.678	Low
NDWI	16.922	Severe

Table S4

Standardized regression coefficients for Model 3.

This table presents standardized beta coefficients describing the relative influence of vegetation cover (NDVI), surface moisture conditions (NDWI), built-up intensity (NDBI_Z), and temporal variables on land surface temperature.

Variable	Estimate	Standardized Beta	Standard Error	t value	P Value
(Intercept)	40.82	NA	0.071	575.39	0.00E+00
NDVI	-28.227	-0.808	0.775	-36.4	6.25E-284
NDBI_Z	1.963	0.47	0.028	69.33	0.00E+00
NDWI	-38.615	-0.972	0.729	-53	0.00E+00
Year2005	2.642	0.238	0.05	53.05	0.00E+00
Year2010	4.442	0.4	0.048	93.47	0.00E+00
Year2015	2.799	0.252	0.047	59.12	0.00E+00
Year2020	5.456	0.491	0.047	115.7	0.00E+00
Year2025	-1.273	-0.115	0.056	-22.64	1.51E-112

Table S5

Year-wise regression model coefficients and adjusted R^2 values.

This table summarizes yearly regression relationships between environmental predictors and land surface temperature across Ahmedabad.

Year	NDVI Coefficient	NDBI Coefficient	NDWI Coefficient	Adjusted R^2
2000	-40.422	1.736	-47.013	0.543
2005	-39.907	1.884	-48.691	0.587
2010	-28.555	1.908	-38.247	0.571
2015	-35.453	1.479	-46.264	0.542
2020	-20.263	2.044	-29.925	0.538
2025	-16.9	2.321	-30.691	0.386

Supplementary Notes

Data and Processing Notes

- Landsat imagery was processed using Google Earth Engine (GEE).
- Thermal and spectral indices were derived from pre-monsoon imagery for each study year.
- NDBI values were standardized independently for each year using z-score normalization.
- Spatial analyses were conducted using Landsat Collection 2 surface reflectance and thermal products.
- Statistical analyses and visualization were conducted in R.

Important Methodological Considerations

- The 2005 Landsat imagery exhibited comparatively lower visual quality relative to other years due to image availability and acquisition constraints.
- Land surface temperature (LST) represents satellite-derived surface thermal conditions and does not directly represent near-surface air temperature or physiological heat exposure.

- Regression coefficients should be interpreted in relation to relative spatial thermal variability rather than direct causality.

Supplementary Code Availability

Google Earth Engine (GEE) scripts and R statistical analysis scripts used in this study are available from the author upon reasonable request.